Eur. Phys. J. C 34, 297–316 (2004)
Digital Object Identifier (DOI) 10.1140/epjc/s2004-01712-x

THE EUROPEAN PHYSICAL JOURNAL C

Exclusive photoproduction of a heavy vector meson in QCD

D.Yu. Ivanov[1], A. Schäfer[2], L. Szymanowski[3], G. Krasnikov[2,4]

[1] Institute of Mathematics, 630090 Novosibirsk, Russia
[2] Institut für Theoretische Physik, Universität Regensburg, 93040 Regensburg, Germany
[3] Soltan Institute for Nuclear Studies, Hoza 69, 00-681 Warsaw, Poland
[4] Department of Theoretical Physics, St. Petersburg State University, 198904, St. Petersburg, Russia

Received: 22 January 2004 /
Published online: 23 March 2004 –

Abstract. The process of exclusive heavy vector meson photoproduction, $\gamma p \to Vp$, is studied in the framework of QCD factorization. The mass of the produced meson, $V = \Upsilon$ or J/Ψ, provides a hard scale for the process. We demonstrate that, in the heavy quark limit and at the one-loop order in perturbation theory, the amplitude factorizes in a convolution of a perturbatively calculable hard-scattering amplitude with the generalized parton densities and the non-relativistic QCD matrix element $\langle O_1 \rangle_V$. We evaluate the hard-scattering amplitude at one-loop order and compare the data with theoretical predictions using an available model for generalized parton distributions.

1 Introduction

The process of elastic production of heavy quarkonium in photon–proton collisions,

$$\gamma p \to Vp\,, \quad \text{where} \quad V = J/\Psi \quad \text{or} \quad \Upsilon\,, \tag{1.1}$$

was studied in fixed target [1, 2] and in HERA collider experiments both for the case of a real photon in the initial state (photoproduction) [3–7] and for the case when the meson is produced by a highly virtual photon (electroproduction) [8, 9]. The primary motivation for the strong interest in this process (and in the similar process of light vector meson electroproduction) is that it can potentially serve to constrain the gluon density in a proton. On the theoretical side, the large mass of the heavy quarks provides a hard scale for the process, which justifies the application of QCD factorization methods that allow one to separate the contributions to the amplitude coming from different scales.

The first step in this direction was made by Ryskin [10], who expressed the amplitude of exclusive heavy meson production in terms of the gluon density and, accordingly, predicted that the cross section, which is proportional to the square of the gluon density, quickly grows with energy. Electroproduction of light vector mesons was studied later in [11], where it was shown that in this case the amplitude factorizes in terms of a perturbative hard-scattering coefficient function and non-perturbative quantities: a meson distribution amplitude and a gluon density in a proton. Again, an increase of the cross section with energy was predicted. The data from HERA appear to be in accord with these predictions.

The early approaches to factorization in exclusive vector meson production [10,11] were based on the use of leading double $\ln(1/x) \ln Q^2$ approximation and were designed for the description of the process at high energies (in the diffractive or small x kinematics). Later on it was understood that in the scaling limit, $Q^2 \to \infty$ and $x = Q^2/W^2$ fixed, deeply virtual meson electroproduction [12] and Compton scattering (DVCS) [13–15] processes may be studied within the QCD collinear factorization method. The proof of factorization for meson electroproduction was provided in [16]. Due to non-vanishing momentum transfer in the t-channel the amplitude of this deeply virtual exclusive process factorizes in terms of generalized parton distributions (GPDs) rather than the ordinary parton densities which enter the QCD description of inclusive deep inelastic scattering and the other hard inclusive processes. GPDs extend the forward parton distributions and the nucleon electromagnetic form factors to the non-forward kinematics of the electroproduction processes, they encode much richer information about the dynamics of a nucleon than the conventional parton distributions. This additional information can be presented e.g. in terms of spatial distributions of energy, spin, ... within a nucleon [17–19]. By now the studies of deeply virtual exclusive processes and GPDs have developed in a very dynamical field; for recent reviews, see [20, 21].

Another QCD approach to exclusive meson production at high energies is related to $k_\perp$ (or high energy) factorization [22,23]; it is based on the BFKL method [24,25]. In this scheme large logarithms of energy $\ln(1/x)$ are resummed and amplitudes are given by an overlap integral of the $k_\perp$ dependent (unintegrated) gluon density and the hard-scattering kernel. High energy factorization can be formulated also in terms of color dipoles [26,27]. Although these

approaches to hard diffractive processes are very promising, their firm foundation, unfortunately, remains limited due to the use of the leading $\ln(1/x)$ approximation. A few years ago the BFKL formalism was extended to the next-to-leading order [28], but the generalization of the $k_\perp$ factorization scheme or the dipole approach to this order remains still a matter of debate. An extended overview of different approaches to this problem may be found in [29].

Most of the theoretical studies [30–38] of process (1.1) were performed in the framework of $k_\perp$ factorization or dipole approaches. Despite great progress and evident success in the description of the data the theoretical uncertainties remain poorly understood. In particular, it is believed that the account of skewedness, i.e. the effect of different parton momentum fractions, is very important for the kinematic range available in the experiment. But since this effect is beyond leading $\ln(1/x)$, its model independent implementation into $k_\perp$ factorization scheme or dipole formalism remains a challenge for the theory.

In this paper we study process (1.1) in the heavy quark limit in the collinear factorization approach. The physics behind collinear factorization is the separation of scales. The mass of the heavy quark, m, provides a hard scale. A photon fluctuates into a heavy quark pair at small transverse distances $\sim 1/m$, which are much smaller than the ones $\sim 1/\Lambda$ related to any non-perturbative hadronic scale Λ. We will show by explicit calculation that to leading power in $1/m$ counting and one-loop order in perturbation theory the amplitude is given by the convolution of the perturbatively calculable hard-scattering amplitude and non-perturbative quantities. The latter are gluon and quark GPDs and the non-relativistic QCD (NRQCD) [39] matrix element $\langle O_1\rangle_V$ which parameterizes in our case the essential non-relativistic dynamics of a heavy meson system. This means that two firmly founded QCD approaches, namely collinear factorization and NRQCD, can be combined to construct a model free description of heavy meson photoproduction which is free of any high energy approximation and may be used also in the kinematic domain where the energy of the photon nucleon collision, W, is of order of the meson mass, M. We evaluate the hard-scattering amplitude at next-to-leading order. This allows us to reduce the scale dependence, which is especially important at high energies, since in this case (i.e. in the small x region) the dependence of the gluon distribution on the scale is very strong.

The factorization theorem [16] for meson electroproduction expresses the amplitude in a form containing a meson light-cone distribution amplitude. Its application to the production of a heavy meson is restricted to the region of very large virtualities, $Q^2 \gg m^2$, where the mass of the heavy quark may be completely neglected. In contrast, in photoproduction or electroproduction at moderate virtualities the heavy quark mass provides a hard scale and the non-relativistic nature of the heavy meson is important. In this case, according to NRQCD, which provides a systematic non-relativistic expansion, a factorization formalism must be constructed in terms of matrix elements of NRQCD operators. They are characterized by their different scaling behavior with respect to v, the typical velocity of the heavy quark. In the leading approximation only the matrix element $\langle O_1\rangle_V$ contributes, which describes in NRQCD the leptonic meson decay rate [39]

$$\Gamma[V \to l^+l^-] = \frac{2e_q^2\pi\alpha^2}{3}\frac{\langle O_1\rangle_V}{m^2}\left(1-\frac{8\alpha_S}{3\pi}\right)^2. \qquad (1.2)$$

Here α is the fine-structure constant and m and e are the pole mass and the electric charge of the heavy quark ($e_c = 2/3, e_b = -1/3$). Equation (1.2) includes the one-loop QCD correction [40] and α_S is the strong coupling constant.

The leading relativistic correction to the meson decay rate and to the photoproduction process (1.1) scales $\sim \langle v^2\rangle$; see [39]. It is expressed through the matrix element of an additional NRQCD operator. Since for a non-relativistic Coulomb system $v \sim \alpha_S$, the relativistic effect is less important than the one-loop perturbative correction. The relativistic correction ($\sim \langle v^2\rangle$) to the result [10] for heavy meson production was studied in [41]; see also [42]. Despite the fact that $\langle v^2\rangle_{J/\Psi} \sim 0.2 \div 0.25$, the relativistic effect was found to be rather small. On the cross section level it amounts to 7% for J/Ψ and it should be even smaller for Υ production.

We will neglect relativistic corrections and consider the process (1.1) in leading order of the relativistic expansion. In this case all essential information about the quarkonium structure is encoded in one NRQCD matrix element. In potential models it can be related to the value of the radial wave function at the origin,

$$\langle O_1\rangle_V = \frac{N_c}{2\pi}|R_S(0)|^2 + \mathcal{O}(v^2), \qquad (1.3)$$

here $N_c = 3$ for QCD. Due to the relation to potential models this scheme of calculation is often called in the literature the static or non-relativistic approximation. However, one should notice that using NRQCD it can be improved in a systematic and rigorous way calculating relativistic and perturbative corrections. In this paper we will concentrate on the one-loop perturbative correction. Our main result is that for this process the collinear factorization method is compatible at one-loop level with the relativistic expansion. This allows us to obtain unambiguous predictions. We found that QCD corrections are large. They change not only the overall normalization but may affect, also, the predictions for the dependence of the cross section on energy.

Our presentation is organized as follows. In Sect. 2 we introduce the notation, discuss the factorization procedure and give the predictions for the amplitude in leading order (LO). Section 3 is devoted to the detailed derivation of the hard-scattering amplitude at next-to-leading order (NLO). Our method is similar to the one we used recently [43] for the calculation of light vector meson electroproduction in NLO. It is based on the use of dispersion relations and the low energy theorem for the radiation of a soft gluon, the non-abelian generalization of the theorem known in QED [44]. In Sect. 4 we present a numerical analysis. In the concluding section we summarize our work and discuss some open questions.

2 Factorization and the amplitude at LO

The kinematics of heavy vector meson photoproduction is shown in Fig. 1. The momenta of the incoming photon, incoming nucleon, outgoing nucleon and the produced meson are q, p, p' and K, respectively. In the leading order of the relativistic expansion the meson mass can be taken as twice the heavy quark pole mass, $K^2 = M^2$ and $M = 2m$. The photon and nucleon are on the mass shell, $q^2 = 0$, $p^2 = p'^2 = m_N^2$, where m_N is the proton mass. The photon polarization is described by the vector e_γ, $(e_\gamma q) = 0$. The invariant CM energy is $s_{\gamma p} = (q+p)^2 = W^2$. We define

$$\Delta = p' - p\,, \quad P = \frac{p+p'}{2}\,, \quad t = \Delta^2\,,$$
$$(q-\Delta)^2 = K^2 = M^2\,, \quad \zeta = \frac{M^2}{W^2}\,. \tag{2.1}$$

In our case the variable ζ has a similar meaning as $x_{\rm Bj}$ in the electroproduction process.

We introduce two light-cone vectors:

$$n_+^2 = n_-^2 = 0\,, \quad n_+ n_- = 1\,. \tag{2.2}$$

Any vector a is decomposed as

$$a^\mu = a^+ n_+^\mu + a^- n_-^\mu + a_\perp\,, \quad a^2 = 2a^+a^- - \mathbf{a}^2\,. \tag{2.3}$$

We choose the light-cone vectors in a similar way as in Ji's notation, namely

$$q = \frac{(W^2 - m_N^2)}{2(1+\xi)W}\, n_-\,,$$
$$p = (1+\xi)W\, n_+ + \frac{m_N^2}{2(1+\xi)W}\, n_-\,,$$
$$p' = (1-\xi)W\, n_+ + \frac{(m_N^2 + \mathbf{\Delta}^2)}{2(1-\xi)W}\, n_- + \Delta_\perp\,,$$
$$\Delta = -2\,\xi\, W\, n_+ + \left(\frac{\xi\, m_N^2}{(1-\xi^2)W} + \frac{\mathbf{\Delta}^2}{2\,(1-\xi)W}\right) n_- + \Delta_\perp\,. \tag{2.4}$$

We are interested in the kinematic region where the invariant transferred momentum,

$$t = \Delta^2 = -\left(\frac{4\,\xi^2}{1-\xi^2} m_N^2 + \frac{1+\xi}{1-\xi}\mathbf{\Delta}^2\right)\,, \tag{2.5}$$

is small, much smaller than m. In the scaling limit the variable ξ which parameterizes the plus component of the momentum transfer equals $\xi = \zeta/(2-\zeta)$.

The amplitude of quarkonium bound state production can be derived from the matrix element which describes the production of the on-shell heavy quark pair, $q_1^2 = q_2^2 = m^2$, $q_1 + q_2 = K$, with a small relative momentum. The explicit equations providing the projection onto quarkonium states with different quantum numbers may be found in [45]. For the S-wave, spin-triplet case, which we are interested in, the procedure corresponds to neglecting the relative momentum of the pair, $q_1 = q_2 = K/2$, and the replacement of the quark spinors by

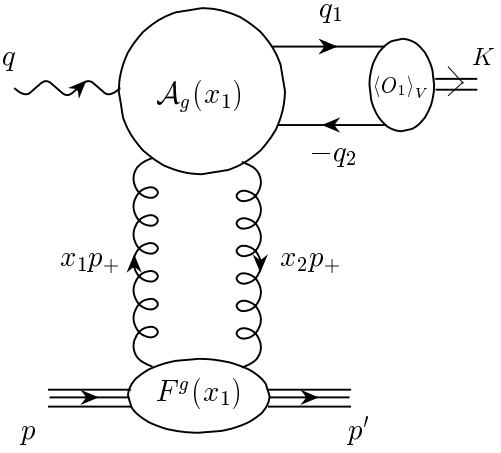

Fig. 1. Kinematics of heavy vector meson photoproduction

$$v_i(q_2)\,\bar u_j(q_1) \to \frac{\delta_{ij}}{4N_c}\left(\frac{\langle O_1\rangle_V}{m}\right)^{1/2} \not{e}_V^*\,(\not{K} + M)\,. \tag{2.6}$$

Here the indices i, j parameterize the color state of the pair, and the vector e_V describes the polarization of the produced vector meson, $(e_V e_V^*) = -1$ and $(K e_V) = 0$.

Collinear factorization states that to leading twist accuracy, i.e. neglecting the contributions which are suppressed by powers of $1/m$, the amplitude can be calculated in the form suggested by Fig. 1:

$$\mathcal{M} = \left(\frac{\langle O_1\rangle_V}{m}\right)^{1/2} \sum_{p=g,q,\bar q} \int_0^1 {\rm d}x_1\, A_{\rm H}^p(x_1,\mu_{\rm F}^2)\, \mathcal{F}_\zeta^p(x_1,t,\mu_{\rm F}^2)\,. \tag{2.7}$$

Here $\mathcal{F}_\zeta^p(x_1,\mu_{\rm F}^2)$ is the gluon or quark GPD in Radyushkin's notation [12]; x_1 and $x_2 = x_1 - \zeta$ are the plus momentum fractions of the emitted and the absorbed partons, respectively. $A_{\rm H}^p(x_1,\mu_{\rm F}^2)$ is the hard-scattering amplitude and $\mu_{\rm F}$ is the (collinear) factorization scale. By definition, GPDs only involve small transverse momenta, $k_\perp < \mu_{\rm F}$, and the hard-scattering amplitude is calculated neglecting the parton transverse momenta. Since quarkonium consists of heavy quarks, it can by produced in LO only by gluon exchange. The Feynman diagrams which describe the LO gluon hard-scattering amplitude are shown in Fig. 2. The contribution of the light quark exchange to quarkonium photoproduction starts in collinear factorization at NLO, it is shown in Fig. 3. Since in this paper we consider the leading helicity non-flip amplitude, in (2.7) the hard-scattering amplitudes $A_{\rm H}^p(x_1,\mu_{\rm F}^2)$ do not depend on t. The account of this dependence would lead to the power suppressed, $\sim t/m$, contribution.

The momentum fraction x_1, $0 \le x_1 \le 1$, is defined with respect to the momentum of the incoming proton. It is convenient to introduce the variable x, $-1 \le x \le 1$, which parameterizes parton momenta with respect to the symmetric momentum $P = (p+p')/2$. The relation between

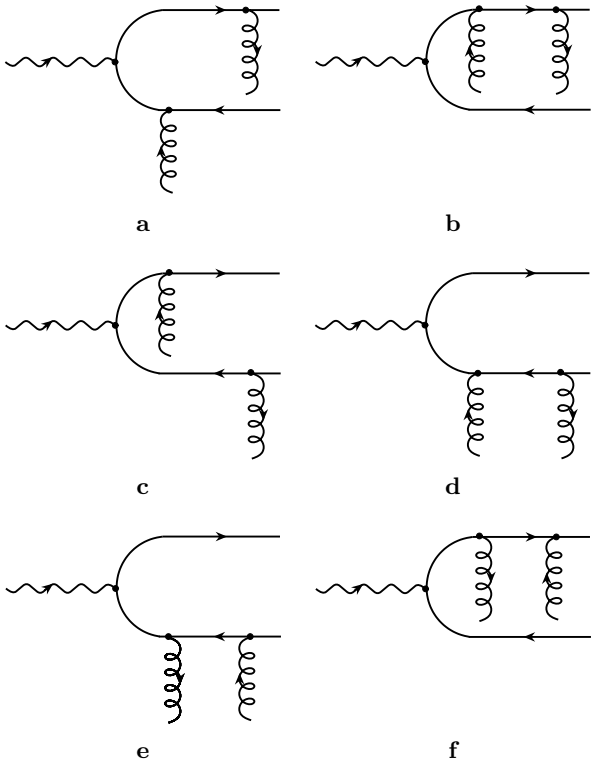

Fig. 2a–f. The hard-scattering amplitude at LO

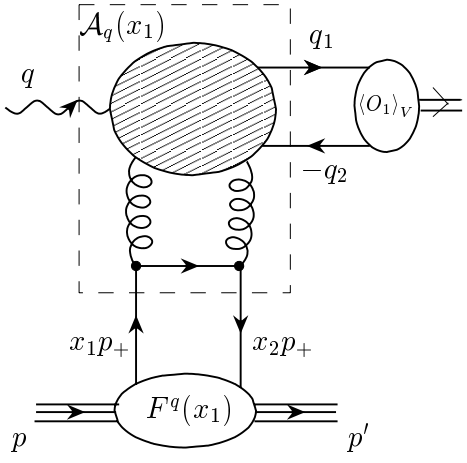

Fig. 3. The light quark contribution to heavy meson photoproduction

the different variables is

$$x_1 = \frac{x+\xi}{1+\xi}\,, \quad x_2 = \frac{x-\xi}{1+\xi}\,. \tag{2.8}$$

In terms of the symmetric variable x the factorization formula reads

$$\mathcal{M} = \frac{4\pi\sqrt{4\pi\alpha}\, e_q(e_V^* e_\gamma)}{N_c\,\xi} \left(\frac{\langle O_1\rangle_V}{m^3}\right)^{1/2} \times \int\limits_{-1}^{1} \mathrm{d}x \left[\, T_g(x,\xi)\, F^g(x,\xi,t) + T_q(x,\xi) F^{q,S}(x,\xi,t)\,\right]\,,$$

$$F^{q,S}(x,\xi,t) = \sum_{q=u,d,s} F^q(x,\xi,t)\,. \tag{2.9}$$

Here the dependence of the GPDs and the hard-scattering amplitudes on μ_F is suppressed for brevity. In the quark contribution the sum runs over all light flavors; see Fig. 3.

GPDs are defined as the matrix element of the renormalized light-cone quark and gluon operators:

$$\begin{aligned} F^q(x,\xi,t) &= \frac{1}{2}\int \frac{\mathrm{d}\lambda}{2\pi} \mathrm{e}^{\mathrm{i}x(Pz)}\, \langle p'|\bar q\left(-\frac{z}{2}\right) \not{n}_- q\left(\frac{z}{2}\right)|p\rangle\Big|_{z=\lambda n_-} \\ &= \frac{1}{2(Pn_-)}\left[\mathcal{H}^q(x,\xi,t)\,\bar u(p')\not{n}_- u(p) \right. \\ &\qquad \left. + \mathcal{E}^q(x,\xi,t)\,\bar u(p')\frac{\mathrm{i}\sigma^{\alpha\beta} n_{-\alpha}\Delta_\beta}{2\,m_N} u(p)\right]\,, \end{aligned} \tag{2.10}$$

$$\begin{aligned} F^g(x,\xi,t) &= \frac{1}{(Pn_-)}\int \frac{\mathrm{d}\lambda}{2\pi} \mathrm{e}^{\mathrm{i}x(Pz)}\, n_{-\alpha} n_{-\beta} \\ &\qquad \times \langle p'|G^{\alpha\mu}\left(-\frac{z}{2}\right) G_\mu^\beta\left(\frac{z}{2}\right)|p\rangle\Big|_{z=\lambda n_-} \\ &= \frac{1}{2(Pn_-)}\left[\mathcal{H}^g(x,\xi,t)\,\bar u(p')\not{n}_- u(p) \right. \\ &\qquad \left. + \mathcal{E}^g(x,\xi,t)\,\bar u(p')\frac{\mathrm{i}\sigma^{\alpha\beta} n_{-\alpha}\Delta_\beta}{2\,m_N} u(p)\right]\,. \end{aligned} \tag{2.11}$$

In both cases the insertion of the path-ordered gauge factor between the field operators is implied. In the LHS of (2.10) and (2.11) the dependence of the GPDs on the normalization point μ_F is suppressed for brevity. In the forward limit, $p' = p$, the contributions proportional to the functions $\mathcal{E}^q(x,\xi,t)$ and $\mathcal{E}^g(x,\xi,t)$ vanish, and the distributions $\mathcal{H}^q(x,\xi,t)$ and $\mathcal{H}^g(x,\xi,t)$ reduce to the ordinary quark and gluon densities:

$$\begin{aligned} &\mathcal{H}^q(x,0,0) = q(x) \quad \text{for} \quad x>0\,, \\ &\mathcal{H}^q(x,0,0) = -\bar q(-x) \quad \text{for} \quad x<0\,; \\ &\mathcal{H}^g(x,0,0) = x\,g(x) \quad \text{for} \quad x>0\,. \end{aligned} \tag{2.12}$$

Note that the gluon GPD is an even function of x,

$$\mathcal{H}^g(x,\xi,t) = \mathcal{H}^g(-x,\xi,t)\,.$$

The definition of the gluon distribution (2.11) involves a field strength tensor and, therefore, is valid in any gauge. But to evaluate the gluon hard-scattering amplitude, it is convenient to consider the light-cone gauge $n_- A = 0$. In this gauge the parton picture which is behind the collinear factorization formalism appears at the level of the individual diagram. One can calculate the contributions of each

gluon diagram separately by considering photon scattering of on-shell gluons with zero transverse momentum and the physical, transverse, polarizations. These gluonic amplitudes have to be multiplied by the light-cone matrix element of two gauge field operators, which has the form [12]

$$\int \frac{\mathrm{d}\lambda(Pn_-)}{2\pi}\,\mathrm{e}^{\mathrm{i}x(Pz)}\,\langle p'|A^a_\mu\left(-\frac{z}{2}\right)A^b_\nu\left(\frac{z}{2}\right)|p\rangle\Big|_{z=\lambda n_-} \quad (2.13)$$
$$= \frac{\delta^{ab}}{N_c^2-1}\left(\frac{-g^\perp_{\mu\nu}}{2}\right)\frac{F^g(x,\xi,t)}{(x-\xi+\mathrm{i}\varepsilon)(x+\xi-\mathrm{i}\varepsilon)}\,.$$

Here a,b are the gluon color indices, $g^\perp_{\mu\nu}=g_{\mu\nu}-n_{+\mu}n_{-\nu}-n_{-\mu}n_{+\nu}$. The $\mathrm{i}\varepsilon$ prescription for the poles in the RHS of (2.13) is important since corresponding singularities lie within the integration domain and contribute to the imaginary part of the amplitude. In simple terms the sign of $\mathrm{i}\varepsilon$ can be understood in this case as being due to the substitution $s\to s+\mathrm{i}\varepsilon$, or $\xi\to\xi-\mathrm{i}\varepsilon$. But one should notice that such an argumentation may not work for more complicated processes which have in their physical regions the absorptive parts in variables other than the energy. For an example and an extended discussion of this issue see [46]. In the case of meson photo- and electroproduction the correct sign of $\mathrm{i}\varepsilon$ is given by (2.13).

The gluon and the quark hard-scattering amplitudes $T_g(x,\xi)$ and $T_q(x,\xi)$ describe the partonic subprocesses

$$\mathcal{A}_g=\mathcal{A}_{\gamma G\to(\bar QQ)G} \quad (2.14)$$

and

$$\mathcal{A}_q=\mathcal{A}_{\gamma q\to(\bar QQ)q}\,, \quad (2.15)$$

respectively. Here Q and q denote the heavy and light quark. We have

$$T_g(x,\xi)=\frac{\xi}{(x-\xi+\mathrm{i}\varepsilon)(x+\xi-\mathrm{i}\varepsilon)}\mathcal{A}_g\left(\frac{x-\xi+\mathrm{i}\varepsilon}{2\xi}\right),$$
$$T_q(x,\xi)=\mathcal{A}_q\left(\frac{x-\xi+\mathrm{i}\varepsilon}{2\xi}\right). \quad (2.16)$$

In the first relation the factor $\xi/((x-\xi+\mathrm{i}\varepsilon)(x+\xi-\mathrm{i}\varepsilon))$ in front of the gluon amplitude comes from the parameterization of the gluon matrix element in the light-cone gauge (2.13).

Partonic amplitudes depend on two independent dimensionful variables, the partonic subenergy $\tilde s=x_1 s$ and the meson mass $M^2=\zeta s$. Being dimensionless quantities the partonic amplitudes can be expressed as a function of the ratio

$$y=\frac{\tilde s-M^2}{M^2}=\frac{x_2}{\zeta}=\frac{x-\xi}{2\xi}\,. \quad (2.17)$$

This convention is adopted in (2.16).

Another Mandelstam variable for the partonic subprocess is $\tilde u=M^2-\tilde s=-x_1 s$. The exchange between the two channels, $\tilde s\leftrightarrow\tilde u$, corresponds to the replacements $x_1\leftrightarrow -x_2$, or $y\leftrightarrow-(1+y)$, or $x\leftrightarrow -x$. Hard scattering amplitudes and GPDs possess definite symmetry properties which are closely related to charge conjugation invariance. A photon and a vector meson have the same C parities, which selects C even exchange in the t-channel. For gluons only a C even GPD exists at leading twist, which is an even function of x, as thus also the gluon hard-scattering amplitude is even in x, $T_g(x,\xi)=T_g(-x,\xi)$. For the quark there exist both C even and C odd GPDs, and F^q has no definite symmetry under the exchange $x\leftrightarrow -x$. But since the quantum numbers of the photon and vector meson select the C even exchange in the t-channel, the quark hard-scattering amplitude obeys $T_q(x,\xi)=-T_q(-x,\xi)$. Therefore only the C even (singlet) component of the quark GPD, $F^{q(+)}=F^q(x,\xi,t)-F^q(-x,\xi,t)$, contributes to (2.9).

Next, we have to evaluate the partonic amplitudes $\mathcal{A}_g$ and $\mathcal{A}_q$. We will use the dimensional regularization method, with $D=4+2\epsilon$ dimensions, in order to regularize the ultraviolet (UV) and infrared (IR) singularities which appear at the intermediate steps of the calculation.

At lowest order there exists only the gluon contribution. $\mathcal{A}_g$ is given by the 6 tree diagrams shown in Fig. 2. A simple calculation gives the result

$$\mathcal{A}_g^{(0)}(y)=\alpha_{\mathrm{S}}(1+\epsilon)\,, \quad (2.18)$$
$$\mathcal{A}_q^{(0)}(y)=0\,. \quad (2.19)$$

The factor $(1+\epsilon)$ in (2.18) appears since in D dimensions there are $2(1+\epsilon)$ transverse polarizations of a gluon. It has to be substituted by 1 when $\mathcal{A}_g^{(0)}$ is inserted in (2.16) to get the LO result for the gluon hard-scattering amplitude. However, we kept this factor in (2.18) since it is important for the correct subtraction of the collinear and ultraviolet counterterms in the NLO amplitudes.

3 The hard-scattering amplitudes at NLO

At LO the gluonic amplitude is a constant; it is a tree amplitude which has no singularities. At NLO the one-loop gluon and quark partonic amplitudes develop a branch cut singularities along the lines $[0,+\infty)$ and $(-\infty,-1]$ in the complex plane of the variable y; see Fig. 4. We will use a method based on the dispersion representation in order to simplify the calculation of these one-loop amplitudes. Deforming the integration contour as shown in Fig. 4 one arrives at a representation of the amplitude which allows one to reconstruct it as a function of the variable y from its discontinuities along the cuts $[0,+\infty)$ and $(-\infty,-1]$. Thanks to the symmetry properties of the partonic amplitudes discussed above the contribution of the branch cut $(-\infty,-1]$ to the dispersion integral may be expressed in terms of the discontinuity at $[0,+\infty)$.

We will start with the quark contribution, then we present the more complicated calculation of the gluonic amplitude. After that we discuss the renormalization and the subtraction of the collinear singularities which lead, finally, to the finite results for the hard-scattering amplitudes at NLO.

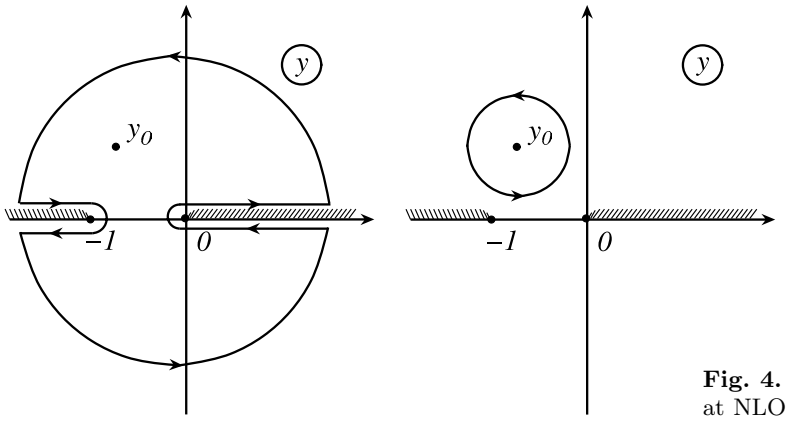

Fig. 4. The analytical properties of the partonic amplitudes at NLO in the complex plane of $y = x_2/\zeta$

3.1 The quark contribution

The dispersion representation for the quark NLO amplitude $\mathcal{A}_q^{(1)}(y)$ reads

$$\mathcal{A}_q^{(1)}(y) = \frac{1}{\pi}\int\limits_0^\infty \mathrm{d}z\, \mathrm{Im}\,\mathcal{A}_q^{(1)}(z)\left(\frac{1}{z-y} - \frac{1}{z+y+1}\right). \tag{3.1}$$

Here $\mathrm{Im}\,\mathcal{A}_q^{(1)}(z)$ stands for the imaginary part of the quark amplitude in the $\tilde{s}$-channel of the quark subprocess. Using the crossing symmetry property, $\mathcal{A}_q(y) = -\mathcal{A}_q(-1-y)$, the contribution of the $\tilde{u}$-channel discontinuity was expressed in terms of $\mathrm{Im}\,\mathcal{A}_q^{(1)}(z)$; it is given by the second term on the RHS of (3.1). For the quark amplitude one can use the unsubtracted dispersion relation, (3.1). $\mathcal{A}_q^{(1)}(z) \sim$ const at large z, but due to cancellation between $\tilde{s}$- and $\tilde{u}$-channel contributions the sum of two terms in the brackets vanishes at large z as $\sim 1/z^2$ while each individual term vanishes as $1/z$. Thus the dispersion integral is convergent at the upper limit. In other words a subtraction constant is not compatible with the symmetry properties of the quark amplitude.

Among the 6 diagrams which contribute to the NLO quark amplitude only 4 diagrams have a discontinuity in the $\tilde{s}$-channel. They are shown in Fig. 5. It is sufficient to calculate the first two diagrams which contain a cut of the light quark and the heavy antiquark lines. The line of the heavy quark in these diagrams is not cut since it enters directly into the meson vertex and, therefore, is effectively on the mass shell. The other two diagrams in Fig. 5 describe the heavy quark cut, their contribution is identical to that one of the first two diagrams.

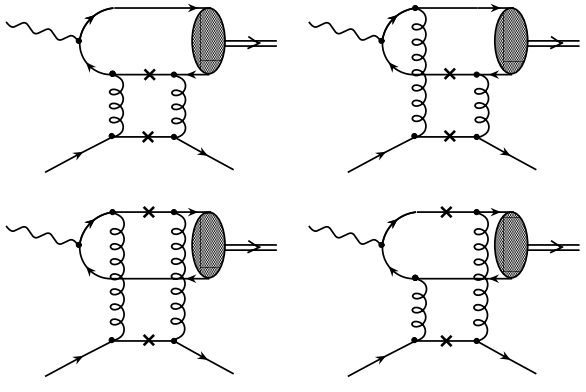

Fig. 5. The $\tilde{s}$-channel cut diagrams for the quark amplitude

We present the quark amplitude in the form

$$\mathcal{A}_q^{(1)}(y) = \frac{\alpha_S^2\, C_F}{(4\pi)^{1+\epsilon}\Gamma(1+\epsilon)}\left(\frac{4m^2}{\mu^2}\right)^{\epsilon}\mathcal{I}_q(y)\,, \tag{3.2}$$

here $\Gamma(\ldots)$ is the Euler gamma function and $C_F = (N_c^2 - 1)/(2N_c) = 4/3$ is the color factor; μ is a scale introduced by dimensional regularization. Calculating the imaginary part we find

$$\begin{aligned}\frac{1}{\pi}\,\mathrm{Im}\,\mathcal{I}_q(y) &= 2\left(\frac{y^2}{1+2y}\right)^{\epsilon} \\ &\times\left(-\frac{1+2y}{1+y}\frac{1}{\epsilon} - \frac{1}{1+2y}\right. \\ &\left. +\frac{3+8y(1+y)}{4y(1+y)}\ln(1+2y)\right).\end{aligned} \tag{3.3}$$

Then, inserting this equation into the dispersion integral (3.1) we obtain the following expression for the quark amplitude:

$$\begin{aligned}\mathcal{I}_q(y) &= \frac{2}{\epsilon}(1+2y)\left(\frac{\ln(-y)}{1+y} - \frac{\ln(1+y)}{y}\right) \\ &- \pi^2\frac{13\,(1+2y)}{24\,y\,(1+y)} + \frac{4\ln 2}{1+2y} + 2\frac{\ln(-y)+\ln(1+y)}{1+2y} \\ &+ 2(1+2y)\left(\frac{\ln^2(-y)}{1+y} - \frac{\ln^2(1+y)}{y}\right) \\ &+ \frac{3-4y+16y(1+y)}{2y(1+y)}\mathrm{Li}_2(1+2y) \\ &- \frac{7+4y+16y(1+y)}{2y(1+y)}\mathrm{Li}_2(-1-2y)\,,\end{aligned} \tag{3.4}$$

where

$$\mathrm{Li}_2(z) = -\int\limits_0^z \frac{\mathrm{d}t}{t}\ln(1-t)\,. \tag{3.5}$$

3.2 The gluon contribution

The analysis of the gluon contribution follows the same lines as for the quark case. However, one has to take into account that the gluonic amplitude is symmetric under crossing, $\mathcal{A}_g(y) = \mathcal{A}_g(-1-y)$, and that the asymptotics of $\mathcal{A}_g^{(1)}(y)$ at large y is $\mathcal{A}_g^{(1)}(y) \sim y$. Therefore we need a dispersion representation of $\mathcal{A}_g^{(1)}(y)$ with one subtraction. It is convenient to perform this subtraction at $y = 0$, the point where the second gluon carries zero energy, since the calculation of the amplitude in this point may be considerably simplified making use of a low energy theorem for the radiation of a soft gluon. The dispersion representation for the gluonic amplitude reads

$$\mathcal{A}_g^{(1)}(y) - \mathcal{A}_g^{(1)}(0) = \frac{1}{\pi}\int\limits_0^\infty \mathrm{d}z\, \mathrm{Im}\,\mathcal{A}_g^{(1)}(z) \times \left(\frac{y}{z(z-y)} - \frac{y}{(z+y)(z+y+1)}\right). \quad (3.6)$$

The second term in the brackets represents the contribution of the $\tilde{u}$-channel cut. Due to cancelation between the $\tilde{s}$- and the $\tilde{u}$-channel contributions the term in the brackets vanishes as $\sim 1/z^3$ rather than as $\sim 1/z^2$ which makes the dispersion integral convergent. Therefore one needs only one subtraction, not two. This can also be expressed in the following manner: the term linear in y of the subtraction polynomial is absent, because it is not compatible with the symmetry property of the gluonic amplitude.

It is convenient to introduce the auxiliary quantity $\mathcal{I}_g(y)$ defined by

$$\mathcal{A}_g^{(1)}(y) = \frac{\alpha_S^2}{(4\pi)^{1+\epsilon}\Gamma(1+\epsilon)}\left(\frac{4m^2}{\mu^2}\right)^\epsilon \mathcal{I}_g(y)\,. \quad (3.7)$$

The imaginary part of the gluonic amplitude may be represented as sum of three different contributions

$$\mathrm{Im}\,\mathcal{I}_g(z) = \mathrm{Im}\,\mathcal{I}_g^{(\bar{Q}Q)}(z) + \mathrm{Im}\,\mathcal{I}_g^{(Qg)}(z) + \mathrm{Im}\,\mathcal{I}_g^{(\bar{Q}g)}(z)\,. \quad (3.8)$$

Here $\mathrm{Im}\,\mathcal{I}_g^{(\bar{Q}Q)}(z)$ represents the sum of 10 diagrams having a $\bar{Q}Q$ cut in the intermediate state; see Figs. 6 and 7. $\mathrm{Im}\,\mathcal{I}_g^{(Qg)}(z)$ gives the contribution of the 24 heavy quark gluon cut diagrams and $\mathrm{Im}\,\mathcal{I}_g^{(\bar{Q}g)}(z)$ is the contribution to the imaginary part coming from the 24 cut diagrams with the heavy antiquark and the gluon in the intermediate state shown in Figs. 8 and 9. The latter two contributions are equal,

$$\mathrm{Im}\,\mathcal{I}_g^{(Qg)}(z) = \mathrm{Im}\,\mathcal{I}_g^{(\bar{Q}g)}(z)\,; \quad (3.9)$$

therefore it is enough to calculate only one of them – say, $\mathrm{Im}\mathcal{I}_g^{(\bar{Q}g)}(z)$. We define the two contributions

$$\mathcal{I}_g(y) - \mathcal{I}_g(0) = \mathcal{I}_g^{(\bar{Q}Q)}(y) + 2\,\mathcal{I}_g^{(\bar{Q}g)}(y)\,, \quad (3.10)$$

in accordance with (3.6), the decomposition of the imaginary part (3.8), and (3.9).

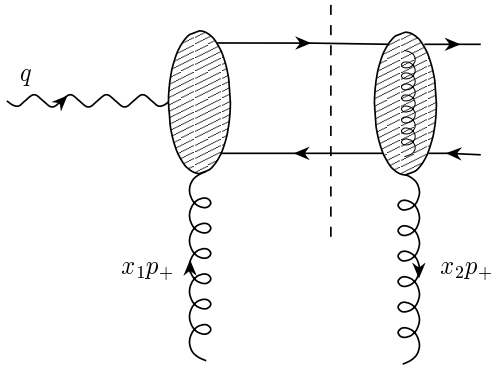

Fig. 6. The contribution of the $\bar{Q}Q$ intermediate state to the gluonic amplitude

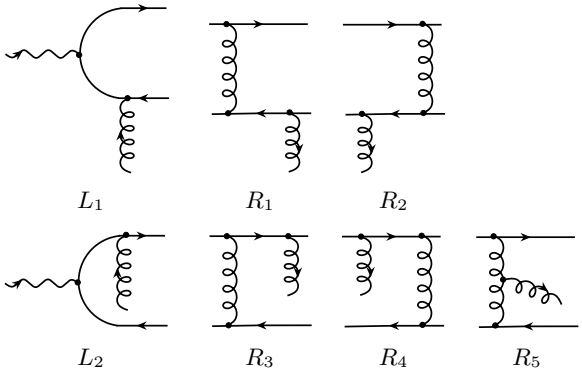

Fig. 7. The left and the right effective vertices for the $\bar{Q}Q$ cut

3.2.1 $\bar{Q}Q$ and $\bar{Q}g$ cut contributions

The calculation of the $\bar{Q}Q$ cut diagrams shown in Figs. 6 and 7 gives

$$\frac{1}{\pi}\mathrm{Im}\,\mathcal{I}_g^{\bar{Q}Q}(y) = (y)^\epsilon \Theta_g^{\bar{Q}Q}(y)\,, \quad (3.11)$$

where

$$\Theta_g^{\bar{Q}Q}(y) = -\frac{\sqrt{y(1+y)}}{y(1+y)}\left(c_1\frac{7}{2} + c_2\left(\frac{3}{y}+1\right)\right) + \frac{\mathrm{arctanh}\sqrt{\frac{y}{1+y}}}{y(1+y)}\left(c_1\left(-\frac{3}{2}+2y\right) + c_2\left(\frac{3}{y}+6+2y\right)\right). \quad (3.12)$$

Here for brevity we denote two independent color structures by

$$c_1 = C_\mathrm{F}\,, \quad c_2 = C_\mathrm{F} - \frac{C_A}{2} = -\frac{1}{2N_c}\,. \quad (3.13)$$

Inserting this result into the dispersion integral (3.6) we obtain

$$\mathcal{I}_g^{\bar{Q}Q}(y) = -5c_1 - \frac{3+2y(1+y)}{y(1+y)}c_2 + \pi\frac{\sqrt{-y(1+y)}}{y(1+y)}\left(\frac{7}{2}c_1 - 3c_2\right)$$

$$
\begin{aligned}
&+\pi^2\left(\frac{3-4y(1+y)}{8y(1+y)}c_1\right.\\
&\qquad\left.-\frac{3+y(1+y)(9-y(1+y))}{4y^2(1+y)^2}c_2\right)\\
&+2c_2\frac{\sqrt{-y(1+y)}}{y(1+y)} \qquad (3.14)\\
&\times\left(\frac{1+4y}{1+y}\arctan\sqrt{\frac{-y}{1+y}}+\frac{3+4y}{y}\arctan\sqrt{\frac{1+y}{-y}}\right)\\
&-\frac{\arctan^2\sqrt{\frac{-y}{1+y}}}{2y(1+y)}\left((7+4y)c_1-2\frac{1+2y-2y^2}{1+y}c_2\right)\\
&-\frac{\arctan^2\sqrt{\frac{1+y}{-y}}}{2y(1+y)}\left((3-4y)c_1-2\frac{3+6y+2y^2}{y}c_2\right).
\end{aligned}
$$

Some words about the calculation of integral (3.6) for $\mathcal{I}_g^{\bar{Q}Q}$ are in order. Since $\mathrm{Im}\,\mathcal{I}_g^{\bar{Q}Q}(z)\sim z^{\epsilon-1/2}$ at small z, the contribution of the region $z\le\delta$ (where $\delta\ll 1$) to the dispersion integral is of the order

$$
\sim\int\limits_0^\delta \mathrm{d}z\, z^{\epsilon-\frac{3}{2}}=\left.\frac{\delta^{\epsilon-\frac{1}{2}}}{\epsilon-\frac{1}{2}}\right|_{\epsilon\to 0}\to-\frac{2}{\sqrt{\delta}}\,. \qquad (3.15)
$$

However, this contribution to $\mathcal{I}_g^{\bar{Q}Q}$, which is singular for $\delta\to 0$, cancels with the one coming from the region $z\ge\delta$ and we arrive at the finite result given by (3.14).

The appearance of integrals like (3.15) is related to a phenomenon well known in quarkonium physics. The gluon exchange between the non-relativistic quark pair contains the Coulomb-like instantaneous contribution. In the NRQCD formalism its contribution has to be subtracted from the hard part of the amplitude. Let us discuss the corresponding counterterm.

In a frame where the $Q\bar{Q}$ system is at rest the momenta of the heavy quarks are

$$
q_1=(m+\varepsilon,\mathbf{p})\,,\quad q_2=(m+E-\varepsilon,-\mathbf{p})\,, \qquad (3.16)
$$

where E denotes the non-relativistic energy of the pair. The LO amplitude has the form

$$
\mathcal{M}^{\mathrm{LO}}=C\int\mathrm{d}\mathbf{p}\,\Psi(\mathbf{p})\,. \qquad (3.17)
$$

Here C is some factor and $\Psi(\mathbf{p})$ is the non-relativistic wave function of the $Q\bar{Q}$ system in momentum representation. The integral (3.17) is proportional to the value of the wave function at the origin

$$
\int\mathrm{d}\mathbf{p}\,\Psi(\mathbf{p})\sim R_S(0)\,. \qquad (3.18)
$$

Now consider the α_{S} correction. The momenta of the quarks after the gluon exchange are

$$
q_1'=(m+\varepsilon',\mathbf{p}')\,,\quad q_2'=(m+E-\varepsilon',-\mathbf{p}')\,. \qquad (3.19)
$$

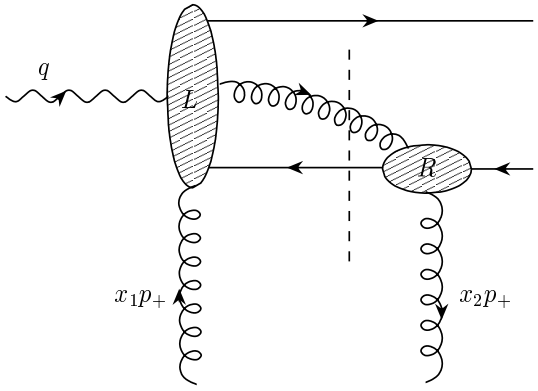

Fig. 8. The contribution of the $\bar{Q}g$ intermediate state to the gluonic amplitude

For the non-relativistic system the energy and the momentum variables scale as $E,\varepsilon,\varepsilon'\sim mv^2$; $|\mathbf{p}|,|\mathbf{p}'|\sim mv$. With NLO accuracy the amplitude can therefore be written as follows

$$
\begin{aligned}
\mathcal{M}^{\mathrm{NLO}}&=C\int\mathrm{d}\mathbf{p}\,\Psi(\mathbf{p})\\
&\times\left(1-\frac{\alpha_{\mathrm{S}}C_{\mathrm{F}}}{2\pi^2(2\pi)^{2\epsilon}}\int\mathrm{d}\mathbf{p}'\frac{1}{(\mathbf{p}-\mathbf{p}')^2\left[E-\frac{\mathbf{p}'^2}{m}+\mathrm{i}0\right]}\right.\\
&\qquad\left.+\mathcal{O}(\alpha_{\mathrm{S}}v^0)\right)\,. \qquad (3.20)
\end{aligned}
$$

The first term on the RHS of (3.20) is the LO contribution, the second and the third terms represent the NLO correction. The latter is finite at $v\to 0$. The second term of (3.20) scales $\sim\alpha_{\mathrm{S}}C_{\mathrm{F}}/v$; it comes from the instantaneous Coulomb exchange. Equation (3.20) can be easily derived considering the integral over the loop momentum, $\mathrm{d}^{4+2\epsilon}q_1'=\mathrm{d}\varepsilon'\mathrm{d}\mathbf{p}'$, and using the non-relativistic limit for the quark propagators. After integration over the loop energy ε' we arrive at the expression given above for the Coulomb contribution. It can be recognized as the exchange potential responsible for the formation of a non-relativistic meson bound state. Indeed, the Schrödinger equation in momentum representation reads

$$
\left(E-\frac{\mathbf{p}'^2}{m}\right)\Psi(\mathbf{p}')=-\frac{\alpha_{\mathrm{S}}C_{\mathrm{F}}}{2\pi^2(2\pi)^{2\epsilon}}\int\mathrm{d}\mathbf{p}\,\frac{\Psi(\mathbf{p})}{(\mathbf{p}-\mathbf{p}')^2}\,. \qquad (3.21)
$$

The second term in (3.20), the Coulomb counterterm, integrated over $\mathrm{d}\mathbf{p}$ produces the LO contribution, $C\int\mathrm{d}\mathbf{p}'\Psi(\mathbf{p}')$, which is already taken into account in the first term. Therefore the Coulomb counterterm has to be subtracted from (3.20). After that one can put the quark pair on the mass shell; $v,E\to 0$, and $\mathbf{p}\to\ 0$.

The advantage of using dimensional regularization is that the quark pair may be put on the mass shell even before the subtraction of the Coulomb counterterm. Since at $E=0$, and $\mathbf{p}=0$ the Coulomb counterterm becomes the scaleless integral, $\sim\int\mathrm{d}\mathbf{p}'/\mathbf{p}'^4\to 0$, it has to be put equal to

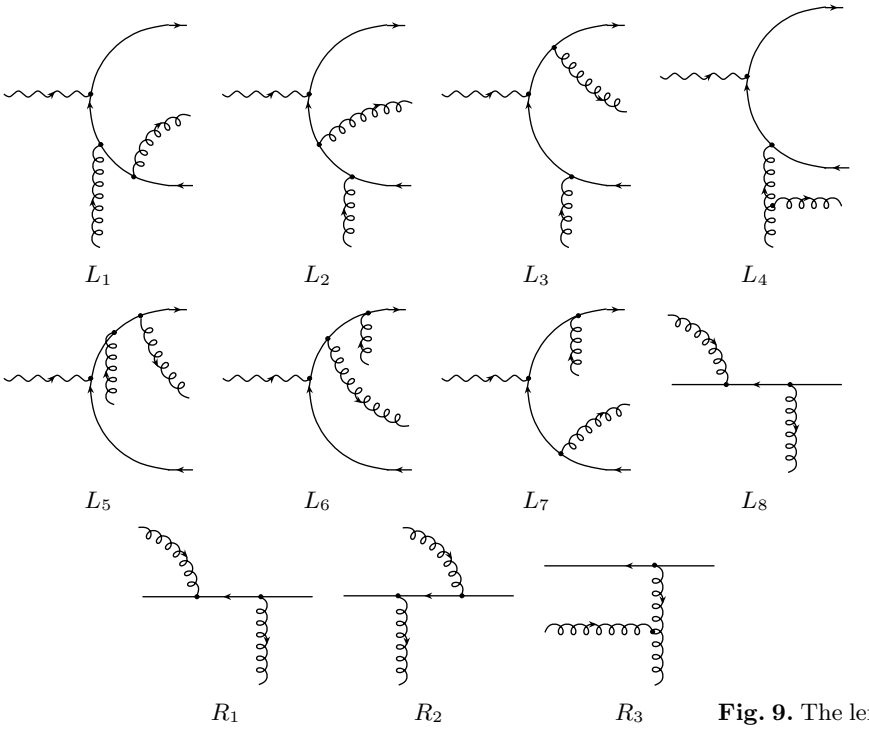

Fig. 9. The left and the right effective vertices for the $\bar{Q}g$ cut

zero according to the rules of the dimensional regularization method. That means that the Coulomb counterterm is zero in this scheme.[1] The price to be paid for the simplification is the appearance of integrals like (3.15). They have to be treated as described above. We encountered integrals of this kind also in the calculation of $\mathcal{I}_g(0)$.

Now we proceed to the calculation of $\mathcal{I}_g^{\bar{Q}g}$. The imaginary part related with the $\bar{Q}g$ cut presented in Figs. 8 and 9 reads

$$\frac{1}{\pi}\mathrm{Im}\,\mathcal{I}_g^{\bar{Q}g}(y) = \left(\frac{y^2}{1+2y}\right)^{\epsilon} \Theta_g^{\bar{Q}g}(y)\,, \tag{3.22}$$

where

$$\begin{aligned}
\Theta_g^{\bar{Q}g}(y) &= -2\frac{1+2y(1+y)}{1+y}\left(\frac{c_1-c_2}{\epsilon}\right) - \frac{5c_1-4c_2}{4} \\
&- 4(c_1-c_2)y + \frac{3c_2}{y} + \frac{3c_1-c_2}{2(1+y)} \\
&+ \frac{5c_1}{4(1+2y)} - \frac{c_1}{4(1+2y)^2} \\
&\quad + \left(\frac{3c_1-4c_2}{2} + 4(c_1-c_2)y \right. \\
&\qquad + \frac{9c_1-22c_2}{8y} + \frac{5c_1-2c_2}{8(1+y)} \\
&\qquad \left. - \frac{c_1}{2(1+2y)} - \frac{3c_2}{4y^2} - \frac{c_1-2c_2}{4(1+y)^2}\right)\ln(1+2y) \\
&- \frac{1}{6}(c_1-c_2)(45-2\pi^2)\epsilon\,.
\end{aligned} \tag{3.23}$$

Expanding $\Theta_g^{\bar{Q}g}(y)$ in ϵ one needs to keep, in the limit of small y, the terms which are up to linear in ϵ, since in the dispersion integral (3.6) they produce the contribution $\sim \epsilon^0$. Calculating the dispersion integral with $\mathrm{Im}\,\mathcal{I}_g^{(\bar{Q}g)}$ we obtain

$$\begin{aligned}
\mathcal{I}_g^{\bar{Q}g}(y) &= \frac{c_1-c_2}{\epsilon^2} \\
&+ \frac{c_1-c_2}{4\epsilon} \\
&\quad \times \left\{1 + 8(1+2y(1+y))\left(\frac{\ln(-y)}{1+y} - \frac{\ln(1+y)}{y}\right)\right\} \\
&- \frac{c_1}{4} + c_2\frac{3+7y(1+y)}{2y(1+y)} \\
&- \pi^2\left[c_1\frac{2+y(1+y)(43+100y(1+y))}{96y^2(1+y)^2}\right. \\
&\qquad \left. - c_2\frac{8+y(1+y)(47+61y(1+y))}{48y^2(1+y)^2}\right] \\
&- \left[c_1\frac{1+2y(1+y)(5+14y(1+y))}{2y(1+y)(1+2y)^2}\right. \\
&\quad \left. + c_2\frac{1+2y(1+y)}{2y(1+y)}\right]\ln(2) \\
&+ 2(c_1-c_2)\big(1+2y(1+y)\big)\left(\frac{\ln^2(-y)}{1+y} - \frac{\ln^2(1+y)}{y}\right) \\
&+ a_1(y)\ln(-y) + a_1(-1-y)\ln(1+y)
\end{aligned} \tag{3.24}$$

[1] We are grateful to Maxim Kotsky for the discussion of this issue.

$$+a_2(y)\mathrm{Li}_2(1+2y)+a_2(-1-y)\mathrm{Li}_2(-1-2y)\,,$$

where the functions a_1 and a_2 are given by the following expressions:

$$a_1(y)=\frac{c_1}{4}\left(5+16y-\frac{6}{1+y}+\frac{1}{(1+2y)^2}-\frac{5}{1+2y}\right) -\frac{c_2}{2}\left(2+\frac{3}{y}+8y-\frac{1}{1+y}\right), \tag{3.25}$$

$$a_2(y)=\frac{c_1}{8} \times\left(12+\frac{9}{y}+64\,y-\frac{2}{(1+y)^2}+\frac{21}{1+y}-\frac{4}{1+2y}\right) -\frac{c_2}{4}\left(8+\frac{3}{y^2}+\frac{11}{y}+32\,y-\frac{2}{(1+y)^2}+\frac{9}{1+y}\right). \tag{3.26}$$

Equations (3.14) and (3.24) define the RHS of (3.10). To finish our consideration of the gluon contribution one still needs to evaluate $\mathcal{I}_g(0)$, the one-loop amplitude describing the emission of a soft gluon.

3.2.2 The emission of a soft gluon

The idea of our method is inspired by the famous result of Low [44], known as the low energy theorem for radiation of a photon. The arguments of Low may be used to constrain the amplitude describing the emission of a soft gluon. In the non-abelian case, due to the confinement phenomenon, the corresponding result has not such a fundamental meaning as in QED. Nevertheless, it can be useful, for problems treatable by perturbative methods. We will first explain the essential steps of our approach for a simple example, namely the calculation of the LO gluonic amplitude (2.18). Then we proceed to the evaluation of $\mathcal{I}_g(0)$.

Let us consider the gluonic process

$$\gamma(q)\,G(x_1p)\to V(K)\,G(x_2p) \tag{3.27}$$

at LO in the limit when the emitted gluon is soft; $x_2\to 0$, $x_1\to\zeta$. With respect to the soft gluon the diagrams in Fig. 2 may be divided into three groups. In diagrams (a) and (b) the soft gluon is radiated from the on-shell quark line, in diagrams (c) and (d) it is attached to the on-shell antiquark line, whereas in diagrams (e) and (f) the soft gluon is emitted from the virtual antiquark and the virtual quark lines, respectively. In the first two cases the quark propagator attached to the soft gluon vertex is close to the mass shell. We call them pole contributions, contrary to the third non-pole case, which describes the emission of the soft gluon from the internal part of the process.[2] Our idea is to calculate the amplitude of the process (3.27) in the soft gluon limit considering the pole contributions only. Below we will show how using gauge invariance the non-pole contributions may be derived from the pole ones.

Neglecting the proton mass and $\Delta_\perp$ one has

$$p=(1+\xi)\,W\,n_+\,,\quad q=\frac{W}{2(1+\xi)}\,n_-\,,\quad K=q+\zeta p\,. \tag{3.28}$$

For the photon polarization vector we choose the gauge $(e_\gamma p)=0$; hence $e_\gamma=e_\gamma^\perp$. Since we are interested in the helicity non-flip amplitude the meson polarization vector can also be chosen transverse, $e_V=e_V^\perp$.

For the process (3.27) in collinear kinematics it happens that for the pole contributions a pole factor $1/x_2$ coming from the denominator of the quark propagator is compensated by the factor x_2 from the nominator. This means that contributions of both the pole and the non-pole diagrams are regular at $x_2\to 0$ and that both classes of diagrams contribute to the amplitude on an equal footing. However in order to apply our method we need to have a pole factor in the pole contributions. For this purpose we change the kinematics of the process (3.27) slightly away from the collinear one introducing the small transverse component to the momenta of the photon and the soft gluon:

$$q\to q'=q+k_\perp\,,\quad x_2p\to k=x_2p+k_\perp\,. \tag{3.29}$$

Note that this replacement makes the photon and the soft gluon lines slightly virtual, $q'^2=k^2=k_\perp^2$. But this effect is quadratic in $k_\perp$ and, therefore, it is small and can be safely neglected, as we will always do below.

The change of the photon momentum (3.29) leads to the following replacement in the expression for the photon polarization vector:

$$e_\gamma=e_\gamma^\perp\to e'_\gamma=e_\gamma^\perp-\frac{(e_\gamma^\perp k_\perp)}{(pq)}\,p\,,\quad (e'_\gamma q')=0\,. \tag{3.30}$$

We denote the polarization vectors of the gluons with momenta x_1p and k by e_g^1 and e_g^2,

$$(e_g^1\,p)=0\,,\quad (e_g^2\,k)=0\,, \tag{3.31}$$

and choose a gauge such that $(e_g^1\,q)=(e_g^2\,q)=0$. Thus, the polarization vector of the first gluon is transverse, $e_g^1=e_g^{1\perp}$, whereas the polarization vector of the soft gluon contains both a transverse and a longitudinal component. e_g^2 is transverse only in the collinear limit: $e_g^2\to e_g^{2\perp}$ at $k_\perp\to 0$.

Let us consider one of the pole diagrams, say, diagram (b). Its contribution to the gluonic amplitude reads

$$A_{(b)}=D\,\mathrm{Sp}\left[\not e_g^2\,\frac{\not K/2+\not k+m}{(K/2+k)^2-m^2}\,\not e_g^1 \times\frac{\not K/2+\not k-x_1\not p+m}{(K/2+k-x_1p)^2-m^2}\,\not e'_\gamma\,\not e_V^*\,(\not K+M)\right]; \tag{3.32}$$

here D is some factor which is irrelevant for our argumentation. The first propagator on the RHS of (3.32) is the propagator of the quark attached to the soft gluon vertex. Its denominator, $(K/2+k)^2-m^2=(kK)$, vanishes in the

[2] Due to color neutrality of the two gluons in the process (3.27) the emission of gluon $G(x_2p)$ from the on-shell line of gluon $G(x_1p)$ is forbidden, thus in our case there is no gluon pole contribution.

soft gluon limit. In accordance with the nominator of this propagator we define two contributions

$$A_{(b)} = A^{\rm add}_{(b)} + A^{z}_{(b)}\,, \tag{3.33}$$

where

$$A^{\rm add}_{(b)} = D\,{\rm Sp}\left[\not e_g^2 \frac{\not K/2+m}{(K/2+k)^2-m^2}\ \not e_g^1 \right.$$
$$\left.\times \frac{\not K/2+\not k-x_1\not p+m}{(K/2+k-x_1p)^2-m^2}\ \not e'_\gamma\ \not e^*_V\,(\not K+M)\right]\,,$$
$$A^{z}_{(b)} = D\,{\rm Sp}\left[\not e_g^2 \frac{\not k}{(K/2+k)^2-m^2}\ \not e_g^1 \right.$$
$$\left.\times \frac{\not K/2+\not k-x_1\not p+m}{(K/2+k-x_1p)^2-m^2}\ \not e'_\gamma\ \not e^*_V\,(\not K+M)\right]\,.$$

Commuting in the first term the factors $\not e_g^2$ and $(\not K/2+m)$ we obtain

$$A^{\rm add}_{(b)} = D\,\frac{(e_g^2K)}{(kK)} \tag{3.34}$$
$$\times\,{\rm Sp}\left[\not e_g^1 \frac{\not K/2+\not k-x_1\not p+m}{(K/2+k-x_1p)^2-m^2}\ \not e'_\gamma\ \not e^*_V\,(\not K+M)\right]\,.$$

The trace on the RHS of (3.34) vanishes linearly in k. Indeed, using the properties of the polarization vectors discussed above it is easy to see that

$$A^{\rm add}_{(b)} = -\frac{D}{m}\,\frac{(e_g^2K)}{(kK)}\,{\rm Sp}\left[\not e_g^1\ \not k\ \not e'_\gamma\ \not e^*_V\right] + \mathcal{O}(k)\,. \tag{3.35}$$

Similarly, for the second term we obtain

$$A^{z}_{(b)} = -\frac{D}{m\,(kK)}\,{\rm Sp}\left[\not e_g^2\ \not k\ \not e_g^1\ \not e'_\gamma\ \not e^*_V\ \not K\right] + \mathcal{O}(k)\,. \tag{3.36}$$

$A^{\rm add}_{(b)}$ vanishes in the collinear kinematics since at $k_\perp \to 0$: $k \to x_2p$, $e_g^2 \to e_g^{2\perp}$ and $(e_g^2K) \to 0$. However, for $k_\perp \neq 0$ both contributions to $A_{(b)}$ are of the same order. Note that $A^{z}_{(b)}$ is finite for $k_\perp = 0$ and $x_2 \to\ 0$.

The consideration of the other pole diagrams follows the same lines. We calculated, similar to (3.35) and (3.36), the corresponding contributions to $A^{\rm add}$ and A^z of each pole diagram. The total gluonic amplitude is

$$A \equiv e_{\rm g}^{2,\,\mu} A_\mu = e_{\rm g}^{2,\,\mu}\left[A^{\rm add}_\mu + A^z_\mu + A^{n-{\rm pole}}_\mu\right]\,, \tag{3.37}$$

where the first two terms represent the pole contributions, and the third term stands for the contribution of the non-pole diagrams. The latter can be obtained from $A^{\rm add}_\mu$ using gauge invariance. Due to current conservation we have

$$k^\mu A_\mu = 0\,. \tag{3.38}$$

Since

$$k^\mu A^z_\mu = 0 \tag{3.39}$$

by construction, see (3.33) and (3.36), we obtain

$$k^\mu A^{\rm add}_\mu = -k^\mu A^{n-{\rm pole}}_\mu\,. \tag{3.40}$$

In its turn $A^{\rm add}_\mu$ has the form

$$A^{\rm add}_\mu = \frac{K_\mu}{(kK)}(kP)\,, \quad P^\mu = \sum_i P^\mu_i\,. \tag{3.41}$$

The vector P receives contributions from the pole diagrams enumerated by the index i. For instance, according to (3.35), the contribution of diagram (b) is

$$P^\mu_{(b)} = -\frac{D}{m}\,{\rm Sp}\left[\not e_g^1\ \not\gamma^\mu\ \not e'_\gamma\ \not e^*_V\right]\,. \tag{3.42}$$

Similarly, we denote the contributions of separate pole diagrams to A^z as A^z_i,

$$A^z = \sum_i A^z_i\,. \tag{3.43}$$

From (3.40) and (3.41) we deduce that

$$A^{n-{\rm pole}}_\mu = -P_\mu\,. \tag{3.44}$$

Thus we have shown how in the soft gluon limit the contribution of the non-pole diagrams can be derived without explicit calculations.

Returning to the collinear kinematics, we have

$$A|_{k_\perp\to 0} = e_g^{2\,\perp,\,\mu}\left[A^z_\mu - P_\mu\right]\big|_{k_\perp\to 0}\,, \tag{3.45}$$

here we used that $A^{\rm add}$ vanishes at $k_\perp \to 0$. Thus, the first term in (3.45) represents the contribution of the pole diagrams in the collinear limit whereas the second term, $\sim P_\mu$, restores the non-pole contribution to the gluonic amplitude in this limit.

Finally, to obtain the gluon hard-scattering amplitude $\mathcal{A}^{(0)}_{\rm g}(y=0)$ one needs to perform the summation over $2+2\epsilon$ transverse polarizations of the gluons ($e^{1\,\perp,\,\mu}_{g,\,\lambda} = e^{2\,\perp,\,\mu}_{g,\,\lambda}$, $\lambda = 1,\ldots,2+2\epsilon$) in the amplitude of the gluonic process $A|_{k_\perp\to 0}$, and then take the limit $x_2 \to\ 0$.

Proceeding separately for each pole diagram with these steps, including the summation over the gluon polarizations, we find

$$\mathcal{A}^{(0)}_{\rm g}(y=0) = \sum_i D_i\,, \quad D_i = D^z_i + D^{\rm add}_i\,, \tag{3.46}$$

where D_i stands for the contribution to the gluon hard-scattering amplitude of the individual diagram. D^z_i and $D^{\rm add}_i$ corresponds to the contribution of the pole diagram i to A^z_μ and P_μ respectively. After a simple calculation we find

$$D^z_{(b)} = D^z_{(d)} = D^{\rm add}_{(b)} = D^{\rm add}_{(d)} = \frac{\alpha_{\rm S}(1+\epsilon)}{4}\,,$$
$$D^z_{(a)} = D^z_{(c)} = D^{\rm add}_{(a)} = D^{\rm add}_{(c)} = 0\,. \tag{3.47}$$

Thus we confirm (2.18). Calculating contributions of the non-pole diagrams (e) and (f) directly one can check that the non-pole contribution is indeed correctly restored by

$\sum_i D_i^{\rm add}$. Although it is very simple this calculation contains all essential points of our method.

Now we proceed with this method to the evaluation of $\mathcal{I}_g(0)$. The one-loop diagrams describing the radiation of a soft gluon from the on-shell antiquark line are shown in Fig. 10. A similar set of diagrams can be drawn for the radiation of the soft gluon from the on-shell quark line. Since these two sets of diagrams transform into one another under the charge parity transformation, it is enough to calculate one of them, say, those in Fig. 10 and then to double the result.

The results of our calculation of the contributions of individual antiquark pole diagrams are summarized in Tables 1 and 2. Using our procedure we obtained for each diagram $D_1, \ldots, D_{11}$ two quantities D_i^z and $D_i^{\rm add}$.[3]

Besides soft and collinear singularities the one-loop gluonic amplitude contains also ultraviolet poles which have to be subtracted in the on-shell scheme. The full renormalization procedure includes mass counterterm diagrams, the renormalization of the heavy quark field and the renormalization of the strong coupling constant. The field and the coupling renormalization will be discussed later, together with the factorization of collinear singularities.

Here we will consider the mass counterterm diagrams. This can be done in our method by considering only mass counterterm diagrams having an antiquark pole in the soft gluon limit. They are shown in Fig. 11. Thus, similar to D_i^z and $D_i^{\rm add}$, we have in Table 2 two contributions for the diagrams C_2 and C_4. Below we show that the sets of diagrams D_{12}, D_{14}, D_{16} and D_{13}, D_{15}, D_{17} together with the mass counterterm diagrams C_1 and C_3 add up to two combinations which are gauge invariant. These sets are the separate gauge invariant contributions which can be calculated, similar to D_i^z, directly in the collinear limit.

At the one-loop level the mass and quark field renormalization constants are equal [47]

$$\frac{\delta m}{m} = \delta Z_2 = -\frac{\alpha_{\rm S}\, C_{\rm F}}{(4\pi)^{1+\epsilon}} \left(\frac{m^2}{\mu^2}\right)^{\epsilon} \left(\frac{3+2\epsilon}{1+2\epsilon}\right) \Gamma[-\epsilon]\,. \quad (3.48)$$

Mass counterterm diagrams are multiplied by $\delta m/m$. Let us consider $\left(D_{12} + C_1 \frac{\delta m}{m} + D_{14} + D_{16}\right)$ and $(D_{13} + C_3 \frac{\delta m}{m} + D_{15} + D_{17})$, which represent the one-loop correction to the soft gluon vertex

$$({\rm i}gt^a) \to ({\rm i}gt^a) \left(1 + \frac{\alpha_{\rm S}\, \Gamma[1-\epsilon]}{(4\pi)^{1+\epsilon}} \left(\frac{m^2}{\mu^2}\right)^{\epsilon} w\right) \not{e}_g^2\,, \quad (3.49)$$

where $w = w_1 + w_2 + w_3$, multiplied by the LO antiquark pole diagrams B_1 and B_2 shown in Fig. 12. After a straightforward calculation we obtain[4]

$w_1 =$ 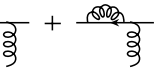

$$= c_1 \left[\frac{3+2\epsilon}{\epsilon(1+2\epsilon)}\right], \quad (3.50)$$

$w_2 =$ 

$$= c_2 \left[-\frac{3+2\epsilon}{\epsilon(1+2\epsilon)} - \frac{\not{k}}{m}\left(\frac{1-2\epsilon}{1+2\epsilon}\right)\right], \quad (3.51)$$

$w_3 =$ 

$$= (c_1 - c_2) \left[-\frac{3+2\epsilon}{\epsilon(1+2\epsilon)} + \frac{\not{k}}{m}\left(\frac{1-\epsilon}{\epsilon(1+2\epsilon)}\right)\right]. \quad (3.52)$$

The sum of these contributions equals

$$w = \left(\frac{c_1 - c_2}{\epsilon} - 3c_1 + 2c_2 + \mathcal{O}(\epsilon)\right) \frac{\not{k}}{m}\,. \quad (3.53)$$

We found that for the one-loop correction to the soft gluon vertex the contributions $\sim \not{e}_g^2$ cancel. What is left is $\sim \not{k}\not{e}_g^2$, which means that the part $\sim \alpha_{\rm S}$ of (3.49) is gauge invariant. Inserting it into the LO diagrams B_1 and B_2 we obtained the results presented in the first two lines of Table 2.

Note that in the abelian case $c_1, c_2 = 1$, and, according to (3.53), the correction to the soft vertex is finite at $\epsilon \to 0$. It corresponds to the contribution of a fermion anomalous magnetic moment, $\alpha/(2\pi)$, which is in accordance with the general statement of Low's theorem in QED. In the non-abelian case this contribution has no such clear physical meaning, since it is infrared divergent.

Finally, summing all contributions in Tables 1 and 2 and multiplying the result by a factor 2 (thus taking into account the quark pole diagrams) we arrive at the following expression for the gluonic amplitude at $x_2 = 0$:

$$\mathcal{I}_g(0) = -2\frac{c_1 - c_2}{\epsilon^2} - \frac{7c_1 - c_2}{2\epsilon} + c_1\left(-\frac{3}{2} + \frac{3\pi^2}{4} + 10\ln(2)\right) - c_2\left(5 + \frac{5\pi^2}{8} + 2\ln(2)\right). \quad (3.54)$$

3.3 NLO results

Let us discuss the structure of singularities of the parton amplitudes. First of all note that, according to (3.10), the double pole terms which are present in (3.54) and (3.24) cancel. Thus, the gluonic amplitude as well as the quark one contains only single poles in ϵ. This means that soft singularities present in the individual contributions cancel in the final expressions for the NLO parton amplitudes. What is left are the single poles in ϵ which, as we show below, represent the ultraviolet and collinear singularities.

[3] The diagrams D_2, D_3 include the instantaneous Coulomb exchange which we treated in dimensional regularization as discussed above.

[4] Note that w_1 is finite for $k \to 0$ only if the mass counterterm diagram is included.

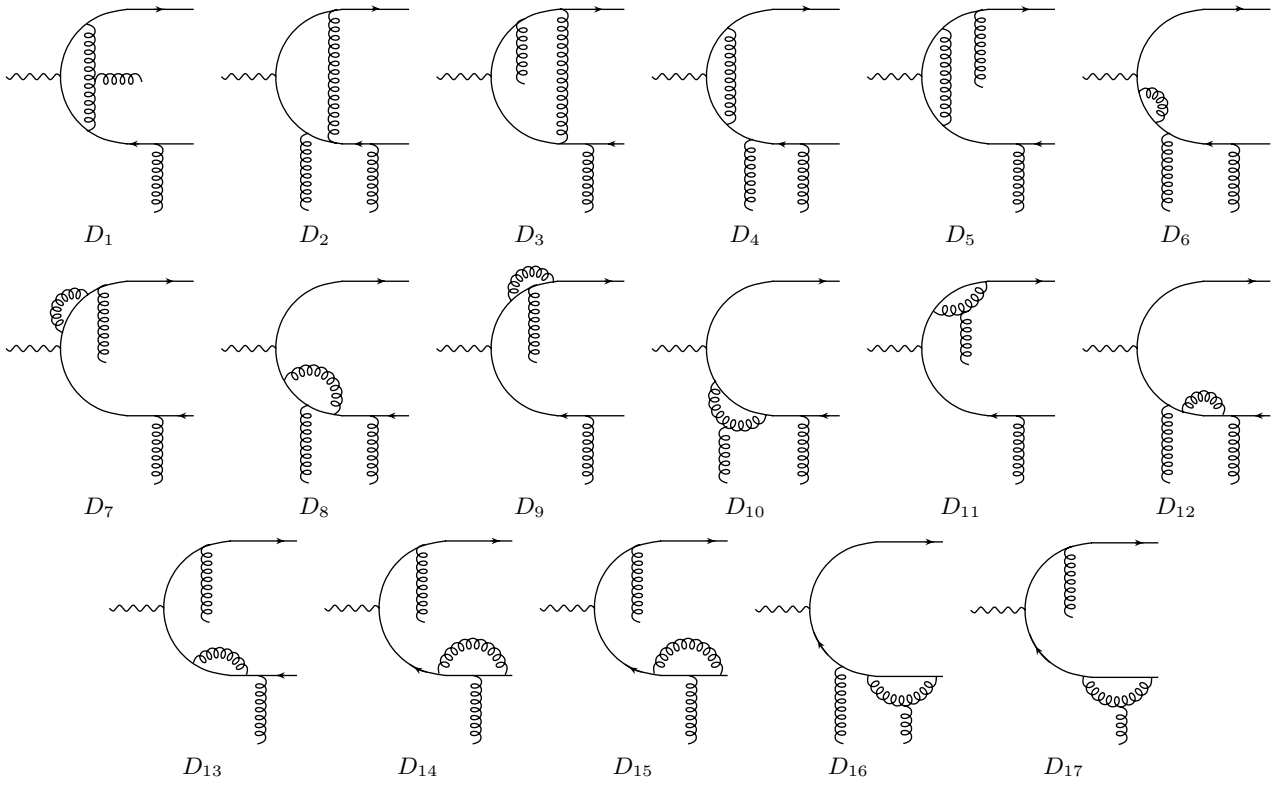

Fig. 10. Diagrams D_i, describing the radiation of a soft gluon from the on-shell antiquark line

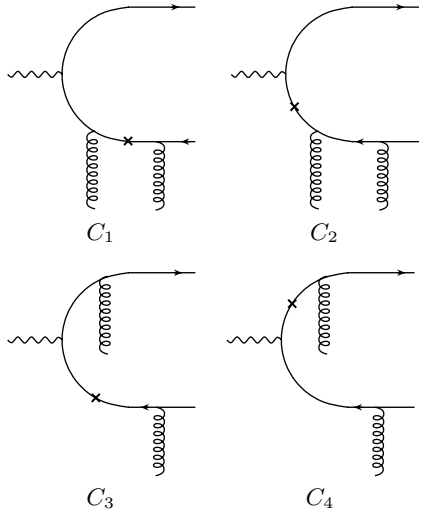

Fig. 11. Mass counterterm diagrams which have an antiquark pole in the soft gluon limit

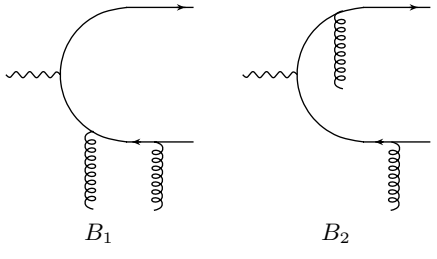

Fig. 12. LO antiquark pole diagrams

To demonstrate the validity of factorization one needs to check that the ultraviolet poles are removed by the heavy quark field and the strong coupling renormalization, and that the collinear poles are absorbed into the quark and gluon GPDs. For this purpose let us recall the structure of the factorization formula

$$\mathcal{M} \sim \int\limits_{-1}^{1} \mathrm{d}x \left[\left(\tilde{T}_g^{(0)}(x,\xi) + \tilde{T}_g^{(1)}(x,\xi) \right) \tilde{F}^g(x,\xi,t) + \tilde{T}_q^{(1)}(x,\xi) \tilde{F}^{q,S}(x,\xi,t) \right] , \tag{3.55}$$

where the tilde indicates that the renormalization and the separation of the collinear singularities has not yet been performed. The bare hard-scattering amplitudes are

$$\begin{aligned} \tilde{T}_g^{(0)}(x,\xi) &= \frac{\xi}{(x-\xi)(x+\xi)} \mathcal{A}_g^{(0)} \left(\frac{x-\xi}{2\xi} \right) \\ &= \frac{\xi}{(x-\xi)(x+\xi)} \alpha_{\mathrm{S}} (1+\epsilon) , \\ \tilde{T}_g^{(1)}(x,\xi) &= \frac{\xi}{(x-\xi)(x+\xi)} \mathcal{A}_g^{(1)} \left(\frac{x-\xi}{2\xi} \right) , \\ \tilde{T}_q^{(1)}(x,\xi) &= \mathcal{A}_q^{(1)} \left(\frac{x-\xi}{2\xi} \right) ; \end{aligned} \tag{3.56}$$

here $\mathcal{A}_q^{(1)}$ is defined by (3.7) and (3.10), and the NLO gluonic amplitude $\mathcal{A}_g^{(1)}$ by (3.7), (3.10), (3.14), (3.24) and (3.54).

Table 1. Contributions to $\mathcal{I}_g(0)$ of diagrams $D_1, \ldots, D_{11}$

Diagram	ϵ^{-2}	ϵ^{-1}	ϵ^0
D_1^z	$-\frac{3}{8}(c_1-c_2)$	$-\frac{3}{8}(c_1-c_2)$	$(c_1-c_2)\left(\frac{\pi^2}{16}+\frac{5\ln(2)}{4}\right)$
$D_1^{\rm add}$	$-\frac{3}{8}(c_1-c_2)$	$-\frac{3}{8}(c_1-c_2)$	$(c_1-c_2)\left(-\frac{1}{2}+\frac{\pi^2}{4}+\frac{7\ln(2)}{2}\right)$
D_2^z	0	$-\frac{1}{4}c_2$	$c_2\left(-\frac{3}{4}+\frac{\pi^2}{32}+\frac{\ln(2)}{2}\right)$
$D_2^{\rm add}$	0	$-\frac{3}{4}c_2$	$c_2\left(-\frac{9}{4}-\frac{3\pi^2}{32}+\frac{13\ln(2)}{4}\right)$
D_3^z	0	0	$c_2\left(-\frac{1}{4}-\frac{\pi^2}{32}+\ln(2)\right)$
$D_3^{\rm add}$	0	0	$c_2\left(\frac{1}{4}+\frac{3\pi^2}{32}-\frac{\ln(2)}{4}\right)$
D_4^z	0	$-\frac{1}{4}c_1$	$c_1\left(-\frac{1}{4}+\frac{\pi^2}{16}\right)$
$D_4^{\rm add}$	0	$-\frac{1}{4}c_1$	$c_1\left(-\frac{1}{8}+\frac{\pi^2}{32}-\frac{\ln(2)}{2}\right)$
D_5^z	0	0	0
$D_5^{\rm add}$	0	0	$c_1\left(\frac{1}{8}-\frac{\pi^2}{32}-\frac{\ln(2)}{2}\right)$
D_6^z	0	$\frac{5}{8}c_1$	$c_1\left(-\frac{1}{8}-\frac{\ln(2)}{4}\right)$
$D_6^{\rm add}$	0	$\frac{13}{16}c_1$	$c_1\left(-\frac{1}{8}-\frac{\ln(2)}{8}\right)$
D_7^z	0	0	$c_1\frac{3}{8}$
$D_7^{\rm add}$	0	$\frac{3}{16}c_1$	$c_1\left(-\frac{3}{8}+\frac{\ln(2)}{8}\right)$
D_8^z	0	$-\frac{1}{4}c_2$	$c_2\left(-\frac{1}{4}+\frac{\pi^2}{16}-\frac{\ln(2)}{2}\right)$
$D_8^{\rm add}$	0	$-\frac{1}{4}c_2$	$c_2\left(\frac{1}{4}-\frac{\pi^2}{16}-\frac{3\ln(2)}{4}\right)$
D_9^z	0	0	0
$D_9^{\rm add}$	0	0	$-c_2\frac{\ln(2)}{4}$
D_{10}^z	$\frac{1}{8}(c_1-c_2)$	$-\frac{3}{8}(c_1-c_2)$	$(c_1-c_2)\left(\frac{1}{2}-\frac{\ln(2)}{2}\right)$
$D_{10}^{\rm add}$	$-\frac{3}{8}(c_1-c_2)$	$-\frac{3}{8}(c_1-c_2)$	$-(c_1-c_2)\left(\frac{1}{2}+\frac{3\ln(2)}{8}\right)$
D_{11}^z	0	0	0
$D_{11}^{\rm add}$	0	0	$-(c_1-c_2)\frac{3\ln(2)}{8}$

Table 2. Contributions to $\mathcal{I}_g(0)$ of $D_{12}, \ldots, D_{17}$ and the mass counterterm diagrams

Diagram	ϵ^{-1}	ϵ^0
$\left(D_{12}+C_1\frac{\delta m}{m}+D_{14}+D_{16}\right)$	$-\frac{1}{4}(c_1-c_2)$	$c_1\left(\frac{1}{2}+\frac{\ln(2)}{2}\right)-c_2\left(\frac{1}{4}+\frac{\ln(2)}{2}\right)$
$\left(D_{13}+C_3\frac{\delta m}{m}+D_{15}+D_{17}\right)$	0	$-(c_1-c_2)\frac{1}{4}$
$C_2^z\frac{\delta m}{m}$	$-\frac{3}{8}c_1$	$c_1\left(\frac{1}{8}+\frac{3\ln(2)}{4}\right)$
$C_2^{\rm add}\frac{\delta m}{m}$	$-\frac{9}{16}c_1$	$c_1\frac{9\ln(2)}{8}$
$C_4^z\frac{\delta m}{m}$	0	$-c_1\frac{3}{8}$
$C_4^{\rm add}\frac{\delta m}{m}$	$-\frac{3}{16}c_1$	$c_1\left(\frac{1}{4}+\frac{3\ln(2)}{8}\right)$

In (3.56) and in some equations below we suppress for brevity the iε prescriptions; they are easily restored by the replacement $\xi \to \xi - {\rm i}\varepsilon$.

The factorization of the collinear singularities corresponds to the substitution, in accordance with the definition of GPDs, of the bare quantities $\tilde{F}^{q,S}(x,\xi,t)$, $\tilde{F}^{g}(x,\xi,t)$ by the renormalized ones. In the modified minimal-subtraction ($\overline{\rm MS}$) scheme one has at the one-loop level

$$\tilde{F}^{q,S}(x,\xi,t) = F^{q,S}(x,\xi,t,\mu_{\rm F}) - \frac{\alpha_{\rm S}(\mu_{\rm F})}{2\pi}\left(\frac{1}{\hat{\epsilon}}+\ln\left(\frac{\mu_{\rm F}^2}{\mu^2}\right)\right)$$

$$\times \int_{-1}^{1} \mathrm{d}v \big[V_{qq}(x,v) F^{q,S}(v,\xi,t,\mu_\mathrm{F}) + V_{qg}(x,v) F^{g}(v,\xi,t,\mu_\mathrm{F}) \big] , \quad (3.57)$$

$$\tilde{F}^g(x,\xi,t) = F^g(x,\xi,t,\mu_\mathrm{F}) - \frac{\alpha_\mathrm{S}(\mu_\mathrm{F})}{2\pi} \left(\frac{1}{\hat{\epsilon}} + \ln\left(\frac{\mu_\mathrm{F}^2}{\mu^2} \right) \right) \times \int_{-1}^{1} \mathrm{d}v \big[V_{gg}(x,v) F^{g}(v,\xi,t,\mu_\mathrm{F}) + V_{gq}(x,v) F^{q,S}(v,\xi,t,\mu_\mathrm{F}) \big] , \quad (3.58)$$

where $V_{qq}, V_{gg}, V_{gq}, V_{qg}$ denote the one-loop evolution kernels. We have

$$\frac{1}{\hat{\epsilon}} = \frac{1}{\epsilon} + \gamma_\mathrm{E} - \ln(4\pi) ; \quad (3.59)$$

γ_E is Euler's constant. Inserting (3.57) and (3.58) into (3.55) and truncating the series at the order α_S^2 we found the following collinear counterterms to the gluon and quark hard-scattering amplitudes

$$\Delta_g^{\mathrm{col}}(x,\xi) = - \frac{\alpha_\mathrm{S}}{2\pi} \left(\frac{1}{\hat{\epsilon}} + \ln\left(\frac{\mu_\mathrm{F}^2}{\mu^2} \right) \right) \int_{-1}^{1} \mathrm{d}v \, \tilde{T}_g^{(0)}(v,\xi) \, V_{gg}(v,x) , \quad (3.60)$$

$$\Delta_q^{\mathrm{col}}(x,\xi) = - \frac{\alpha_\mathrm{S}}{2\pi} \left(\frac{1}{\hat{\epsilon}} + \ln\left(\frac{\mu_\mathrm{F}^2}{\mu^2} \right) \right) \int_{-1}^{1} \mathrm{d}v \, \tilde{T}_g^{(0)}(v,\xi) \, V_{gq}(v,x) . \quad (3.61)$$

Note that, since $\tilde{T}_q^{(0)} = 0$ for our process, the renormalization of the quark GPD (3.57) does not generate contributions ($\sim V_{qq}, V_{qg}$) to the collinear counterterms. Calculating the integrals (3.60) and (3.61) with these kernels we obtain

$$\Delta_g^{\mathrm{col}}(x,\xi) = - \frac{\alpha_\mathrm{S}^2}{2\pi} \frac{\xi}{(x-\xi)(x+\xi)} \left(\frac{1}{\hat{\epsilon}} + 1 + \ln\left(\frac{\mu_\mathrm{F}^2}{\mu^2} \right) \right) \times \left[N_c \, \mathcal{C}_g\left(\frac{x-\xi}{2\xi} \right) + \frac{\beta_0}{2} \right] , \quad (3.62)$$

$$\Delta_q^{\mathrm{col}}(x,\xi) = - \frac{\alpha_\mathrm{S}^2}{2\pi} \left(\frac{1}{\hat{\epsilon}} + 1 + \ln\left(\frac{\mu_\mathrm{F}^2}{\mu^2} \right) \right) C_\mathrm{F} \, \mathcal{C}_q\left(\frac{x-\xi}{2\xi} \right) , \quad (3.63)$$

where

$$\beta_0 = \frac{11 \, N_c}{3} - \frac{2 \, n_f}{3} ; \quad (3.64)$$

n_f is an effective number of light quark flavors, and

$$\mathcal{C}_g(y) = (1 + 2y(y+1)) \left(\frac{\ln(-y)}{1+y} - \frac{\ln(1+y)}{y} \right) ,$$

$$\mathcal{C}_q(y) = (1+2y) \left(\frac{\ln(-y)}{1+y} - \frac{\ln(1+y)}{y} \right) . \quad (3.65)$$

For the renormalization of the strong coupling one has to substitute the bare coupling constant α_S by the running coupling $\alpha_\mathrm{S}(\mu_\mathrm{R})$ in the $\overline{\mathrm{MS}}$ scheme,

$$\alpha_\mathrm{S} = \alpha_\mathrm{S}(\mu_\mathrm{R}) \left[1 + \frac{\alpha_\mathrm{S}(\mu_\mathrm{R})}{4\pi} \beta_0 \left(\frac{1}{\hat{\epsilon}} + \ln\left(\frac{\mu_\mathrm{R}^2}{\mu^2} \right) \right) \right] . \quad (3.66)$$

This substitution generates the following counterterm to the gluon hard-scattering amplitude:

$$\Delta_g^{\alpha_\mathrm{S}}(x,\xi) = \frac{\alpha_\mathrm{S}^2}{4\pi} \frac{\xi}{(x-\xi)(x+\xi)} \left(\frac{1}{\hat{\epsilon}} + 1 + \ln\left(\frac{\mu_\mathrm{R}^2}{\mu^2} \right) \right) \beta_0 . \quad (3.67)$$

To account for the heavy quark field renormalization effect one has to add the counterterm

$$\Delta_g^{Z_2}(x,\xi) = \delta Z_2 \, \tilde{T}_g^{(0)}(x,\xi) , \quad (3.68)$$

with δZ_2 given in (3.48).

In the sum of the bare hard-scattering amplitudes and the counterterms described above all poles in ϵ cancel. Thus, we can now take the limit $\epsilon \to 0$:

$$T_g(x,\xi) = \Big[\tilde{T}_g(x,\xi) + \Delta_g^{\mathrm{col}}(x,\xi) + \Delta_g^{\alpha_\mathrm{S}}(x,\xi) + \Delta_g^{Z_2}(x,\xi) \Big]_{\epsilon\to 0} ,$$
$$T_q(x,\xi) = \Big[\tilde{T}_q(x,\xi) + \Delta_q^{\mathrm{col}}(x,\xi) \Big]_{\epsilon\to 0} , \quad (3.69)$$

and arrive at finite results for the hard-scattering amplitudes:

$$T_q(x,\xi) = \frac{\alpha_\mathrm{S}^2(\mu_\mathrm{R}) C_\mathrm{F}}{2\pi} f_q\left(\frac{x-\xi+\mathrm{i}\varepsilon}{2\xi} \right) , \quad (3.70)$$

$$\begin{aligned} f_q(y) &= \left(\ln\frac{4m^2}{\mu_\mathrm{F}^2} - 1 \right) (1+2y) \left(\frac{\ln(-y)}{1+y} - \frac{\ln(1+y)}{y} \right) \\ &- \pi^2 \frac{13(1+2y)}{48y(1+y)} + \frac{2\ln 2}{1+2y} + \frac{\ln(-y)+\ln(1+y)}{1+2y} \\ &+ (1+2y) \left(\frac{\ln^2(-y)}{1+y} - \frac{\ln^2(1+y)}{y} \right) \\ &+ \frac{3-4y+16y(1+y)}{4y(1+y)} \mathrm{Li}_2(1+2y) \\ &- \frac{7+4y+16y(1+y)}{4y(1+y)} \mathrm{Li}_2(-1-2y) \end{aligned} \quad (3.71)$$

for the quark, and

$$T_g(x,\xi) = \frac{\xi}{(x-\xi+\mathrm{i}\varepsilon)(x+\xi-\mathrm{i}\varepsilon)} \times \left[\alpha_\mathrm{S}(\mu_\mathrm{R}) + \frac{\alpha_\mathrm{S}^2(\mu_\mathrm{R})}{4\pi} f_g\left(\frac{x-\xi+\mathrm{i}\varepsilon}{2\xi} \right) \right] , \quad (3.72)$$

$$
\begin{aligned}
&f_g(y)\\
&= 4(c_1-c_2)\big(1+2y(1+y)\big)\left(\frac{\ln(-y)}{1+y}-\frac{\ln(1+y)}{y}\right)\\
&\times\left(\ln\frac{4m^2}{\mu_{\rm F}^2}-1\right)+\beta_0\ln\frac{\mu_{\rm R}^2}{\mu_{\rm F}^2}\\
&+4(c_1-c_2)\big(1+2y(1+y)\big)\left(\frac{\ln^2(-y)}{1+y}-\frac{\ln^2(1+y)}{y}\right)\\
&-8c_1\\
&-\pi^2\left(\frac{2+y(1+y)(25+88y(1+y))}{48y^2(1+y)^2}c_1\right.\\
&\qquad\left.+\frac{10+y(1+y)(7-52y(1+y))}{24y^2(1+y)^2}c_2\right)\\
&-\left[c_1\frac{1+6y(1+y)(1+2y(1+y))}{y(1+y)(1+2y)^2}\right.\\
&\quad\left.+c_2\frac{(1+2y)^2}{y(1+y)}\right]\ln(2)\\
&+\pi\frac{\sqrt{-y(1+y)}}{y(1+y)}\left(\frac{7}{2}c_1-3c_2\right)\\
&+2c_2\frac{\sqrt{-y(1+y)}}{y(1+y)}\\
&\quad\times\left(\frac{1+4y}{1+y}\arctan\sqrt{\frac{-y}{1+y}}+\frac{3+4y}{y}\arctan\sqrt{\frac{1+y}{-y}}\right)\\
&-\frac{\arctan^2\sqrt{\frac{-y}{1+y}}}{2y(1+y)}\left((7+4y)c_1-2\frac{1+2y-2y^2}{1+y}c_2\right)\\
&-\frac{\arctan^2\sqrt{\frac{1+y}{-y}}}{2y(1+y)}\left((3-4y)c_1-2\frac{3+6y+2y^2}{y}c_2\right)\\
&+2\,a_1(y)\ln(-y)+2\,a_1(-1-y)\ln(1+y)\\
&+2\,a_2(y){\rm Li}_2(1+2y)+2\,a_2(-1-y){\rm Li}_2(-1-2y)
\end{aligned}
\tag{3.73}
$$

for the gluon. $a_1(y), a_2(y)$ are defined in (3.25) and (3.26). The expressions in (3.70)–(3.73) represent the main result of this paper.

At high energies, $W^2 \gg M^2$, the imaginary part of the amplitude dominates. The leading contribution to the NLO correction comes from the integration region $\xi \ll |x| \ll 1$. Simplifying the gluon (3.73) and the quark (3.71) hard-scattering amplitudes in this limit we obtain the estimate

$$
\begin{aligned}
\mathcal{M} &\approx \frac{-4\,{\rm i}\,\pi^2\sqrt{4\pi\alpha}\,e_q(e_V^* e_\gamma)}{N_c\,\xi}\left(\frac{\langle O_1\rangle_V}{m^3}\right)^{1/2}\\
&\times\left[\alpha_{\rm S}(\mu_{\rm R})F^g(\xi,\xi,t)\right.\\
&+\frac{\alpha_{\rm S}^2(\mu_{\rm R})N_c}{\pi}\ln\left(\frac{m^2}{\mu_{\rm F}^2}\right)\int\limits_\xi^1\frac{{\rm d}x}{x}F^g(x,\xi,t)\\
&+\frac{\alpha_{\rm S}^2(\mu_{\rm R})C_{\rm F}}{\pi}\left(\ln\left(\frac{m^2}{\mu_{\rm F}^2}\right)-1\right)\\
&\left.\times\int\limits_\xi^1{\rm d}x\left(F^{q,S}(x,\xi,t)-F^{q,S}(-x,\xi,t)\right)\right].
\end{aligned}
\tag{3.74}
$$

Given the behavior of the gluon and the quark GPDs at small x, $F^g(x,\xi,t)\sim$ const and $F^{q,S}(x,\xi,t)\sim 1/x$, we see from (3.74) that the relative value of the NLO correction is parameterically large at small ξ,

$$
\begin{aligned}
&\sim\frac{\alpha_{\rm S}(\mu_{\rm R})N_c}{\pi}\ln\left(\frac{1}{\xi}\right)\left[\ln\left(\frac{m^2}{\mu_{\rm F}^2}\right)\right.\\
&\left.+\frac{C_{\rm F}}{N_c}\left(\ln\left(\frac{m^2}{\mu_{\rm F}^2}\right)-1\right)\frac{F^{q,S}(\xi,\xi,t)-F^{q,S}(-\xi,\xi,t)}{F^g(\xi,\xi,t)}\right].
\end{aligned}
\tag{3.75}
$$

The gluon correction in (3.75) is negative unless one chooses a value of the factorization scale $\mu_{\rm F} < m$, which is substantially smaller than the kinematic scale $M = 2m$. The quark correction is also parameterically large at high energies. It is expected to be sizable since it collects the contributions of all the light quarks and antiquarks. These qualitative observations are supported by the numerical analysis.

4 Numerical analysis

We assume as values of the quark pole masses $m_c = 1.5\,{\rm GeV}$, $m_b = 4.9\,{\rm GeV}$. $\langle O_1\rangle_V$ was evaluated using (1.2) with $\alpha_{\rm S} = \alpha_{\rm S}(\mu_{\rm R})$. For the generalized parton distributions we adopt the parameterizations, evolved both in LO and NLO, of [48] that are based on the CTEQ6 set of forward distributions [49]. We neglect the contributions proportional to $\mathcal{E}^g(x,\xi,t)$ and $\mathcal{E}^g(x,\xi,t)$. In the numerical calculations we use LO strong running coupling and LO GPDs and NLO coupling and NLO GPDs for LO and NLO observables correspondingly.

Let us start with Υ photoproduction. We calculate with our formulas the forward amplitude and the forward differential cross section, ${\rm d}\sigma/{\rm d}\Delta_\perp^2$ at $\Delta_\perp = 0$. For the $\Delta_\perp$ dependence we assume, in accordance with the measurements at HERA, the simple exponential

$$
\frac{{\rm d}\sigma}{{\rm d}\Delta_\perp^2} = \left(\left.\frac{{\rm d}\sigma}{{\rm d}\Delta_\perp^2}\right|_{\Delta_\perp=0}\right){\rm e}^{-b\boldsymbol{\Delta}_\perp^2},\quad \sigma = \frac{1}{b}\left(\left.\frac{{\rm d}\sigma}{{\rm d}\Delta_\perp^2}\right|_{\Delta_\perp=0}\right).
\tag{4.1}
$$

For the slope parameter we use $b = 4.4\,{\rm GeV}^{-2}$.

In Fig. 13 the LO predictions for the total cross section of Υ photoproduction are shown as a function of energy, the data points are from ZEUS [5] and H1 [6]. The curves correspond to different values of the factorization scale $\mu_{\rm F}$ which is chosen equal to $\mu_{\rm R}$. The experimental uncertainties are large. We find that for the broad interval of scales,

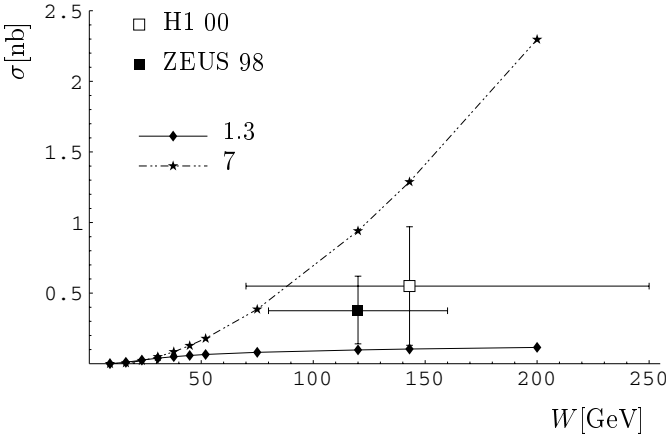

Fig. 13. The cross section for Υ photoproduction; the theoretical predictions at LO for the scales $\mu_F = \mu_R = [1.3, 7]$ GeV (ranging from bottom to top), and the data are from ZEUS [5] and H1 [6]

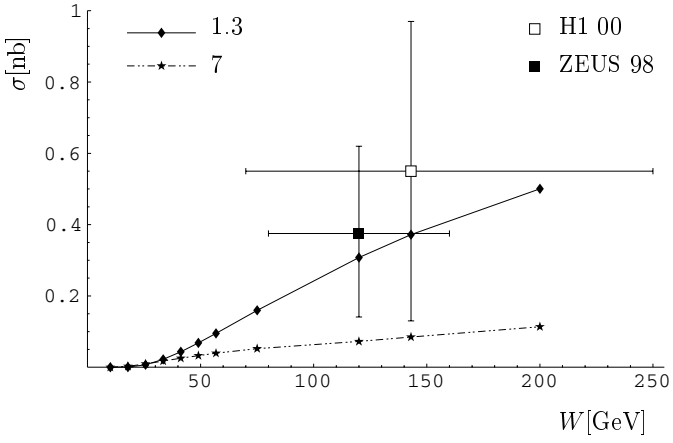

Fig. 14. The cross section of the Υ photoproduction; theoretical predictions at NLO for the scales $\mu_F = \mu_R = [1.3, 7]$ GeV (ranging from top to bottom), and the data from ZEUS [5] and H1 [6]

$\mu_F = \mu_R = 1.3 \div 7$ GeV, our LO predictions lie within the experimental error bars. The strong dependence of the predictions on the factorization scale is related to the well known fact that scaling violation is large for small x. At small x the gluon density increases rapidly with growing μ_F which leads to an increase of the LO predictions with μ_F. In Fig. 14 we present the results of the NLO calculations for the same set of scales. For meson production in NLO this effect is partially compensated, as it should be, due to the dependence of the gluon and the quark hard-scattering NLO amplitudes on μ_F; see (3.70)–(3.73). As a result we observe a substantial reduction of the scale ambiguity of the theoretical predictions in NLO in comparison with LO.

The NLO predictions are generally smaller than the LO ones. The reason is twofold. First, according to the parameterizations we use, in this kinematic region the gluon GPD in NLO is about a factor of two smaller than the gluon GPD in the LO. This is another manifestation of the large scaling violation effects at small x. Second, we find, in accordance with the estimate (3.74), that the part of the gluon NLO hard-scattering amplitude (3.72) $\sim \alpha_S^2$ leads to a contribution which is large and has at $\mu_F \gtrsim m$ a sign opposite to the one of the contribution $\sim \alpha_S$ induced by the Born term of (3.72). The last statement is illustrated in Fig. 15 where the different contributions to the NLO result for $\mu_F = \mu_R = 4.9$ GeV are shown. In the left upper panel we present the cross section. Here the curve labeled Born represents the results calculated using only the Born term of (3.72), the other curve, labeled total, is the cross section calculated with the complete result for the NLO hard-scattering amplitudes, including the quark contribution. To avoid misunderstanding, in both calculations the NLO GPDs were used. We see that the parts of the NLO hard-scattering amplitudes $\sim \alpha_S^2$ make the cross section significantly smaller. On the bottom left and the bottom right panels of Fig. 15 we present the decomposition into different contributions of the imaginary and the real parts of the NLO amplitude divided by its absolute value, $\mathrm{Im}\,\mathcal{M}/|\mathcal{M}|$ and $\mathrm{Re}\,\mathcal{M}/|\mathcal{M}|$. The curves labeled total represent the results calculated with the complete NLO hard-scattering amplitudes (3.72) and (3.70). In these figures the quark contribution and the decomposition of the gluon contribution into the Born and the part induced by the term$\sim \alpha_S^2$ of (3.72) are shown separately. The corresponding curves are labeled as "quark", "Born" and "gluon". In the right upper panel we show $\mathrm{Im}\,\mathcal{M}/|\mathcal{M}|$ and $\mathrm{Re}\,\mathcal{M}/|\mathcal{M}|$ together. We see that, despite the fact that the value of a strong coupling constant is small at this scale, $\alpha_S(\mu_R)/(2\pi) \sim 0.033$ at $\mu_R = 4.9$ GeV, the gluon correction constitutes $\sim 30\%$ of the Born contribution with the opposite sign. The quark contribution is about $\sim 15\%$, with the opposite sign with respect to the Born contribution. Note also that at high energies the imaginary part of the amplitude is about twice the real part.

The reduction of the ambiguity for the theoretical predictions due to a variation of μ_F is even more pronounced if one chooses a fixed value of renormalization scale; see Fig. 16. In this case the value of the cross section is predicted to be smaller than for equal scales, $\mu_R = \mu_F$; compare Figs. 16 and 14.

To summarize our results for Υ photoproduction we conclude that the NLO corrections stabilize the theoretical predictions with respect to variation of the factorization scale. The NLO corrections are numerically important. They make the NLO cross sections smaller than the LO ones, and for the GPD model used our results seem to lie somewhat below the data.

For the photoproduction of J/Ψ the situation is different than for Υ production since in this case a value of the hard scale, the quark mass, is smaller. The NLO corrections are much larger than in the case of Υ production for the following two reasons. First, the value of the QCD running coupling is larger at smaller scales. Second, the value of ξ and, consequently, the effective values of x in the factorization formula is about two orders of magnitude smaller than for Υ production. Therefore the effect of the enhancement of the NLO correction at small x, see (3.74) and (3.75), is much larger for J/Ψ. This is illustrated in Fig. 17 where

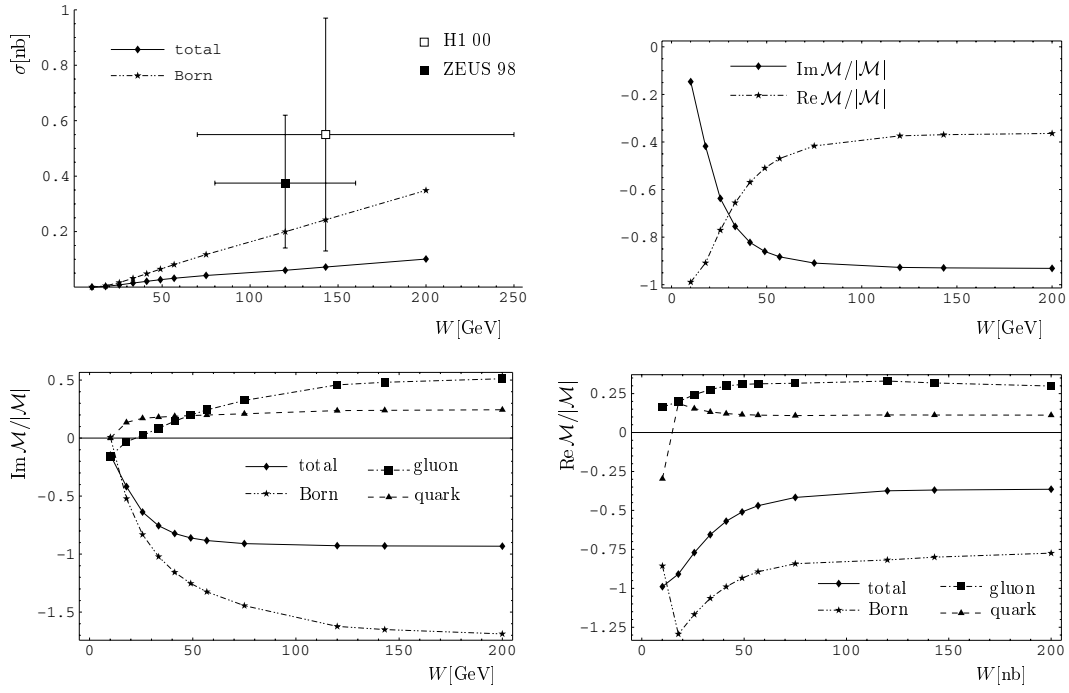

Fig. 15. Υ photoproduction, NLO prediction for $\mu_F = \mu_R = 4.9\,\text{GeV}$ and its decomposition into different contributions; see text

the labeling of the curves is the same as in Fig. 15. The data are from E401 [1] and ZEUS [7]. Note that, contrary to Fig. 15, in the left upper panel of Fig. 17 the results for the forward differential cross section are shown. We see that although the predictions for the cross section are in reasonable agreement with the data, the absolute value of the NLO correction is very large. Note also that in this case the quark GPD makes a significant contribution. The sum of the gluon and the quark NLO corrections is as much as twice the Born contribution and of opposite sign. Therefore in NLO the total amplitude has the opposite sign as in LO. Note also that the imaginary part of the NLO amplitude goes through zero at $W \sim 25\,\text{GeV}$, which is unnatural. Thus, we conclude that for the J/Ψ photoproduction the higher order corrections are not under control.

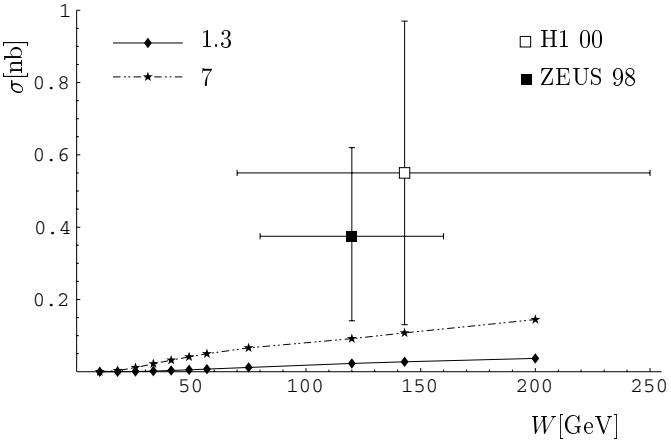

Fig. 16. The cross section for Υ photoproduction, and NLO predictions for the scales $\mu_F = [1.3, 7]\,\text{GeV}$, $\mu_R = 5.9\,\text{GeV}$

5 Summary

We have shown by an explicit calculation of the partonic one-loop amplitudes that in the heavy quark limit the collinear factorization and the non-relativistic QCD approach applied to quarkonium photoproduction are compatible and lead to the unambiguous predictions (3.70)–(3.73) for the hard-scattering amplitudes in the NLO. Presumably such a factorization scheme can be generalized to all orders of the strong coupling expansion. The study of this issue, although very interesting, goes beyond the scope of the present paper.

The numerical analysis for the Υ photoproduction shows that in comparison to LO the NLO corrections to the hard-scattering amplitudes reduce significantly the ambiguity of the predictions related to the choice of factorization scale. The NLO corrections are large, at HERA energies they constitute about $\sim 40\%$ of the Born contribution at the amplitude level and are of the opposite sign compared to the Born contribution.

Contrary to that, we find that for the photoproduction of J/ψ in HERA kinematics the magnitude of the NLO correction is about two times larger than the Born contribution. Also we observe a very strong dependence of the theoretical predictions on μ_F. That forces us to conclude that at high energies for J/ψ photoproduction these corrections are not under theoretical control if one works in NLO, i.e. in the collinear factorization scheme truncated at the second order of the strong coupling expansion.

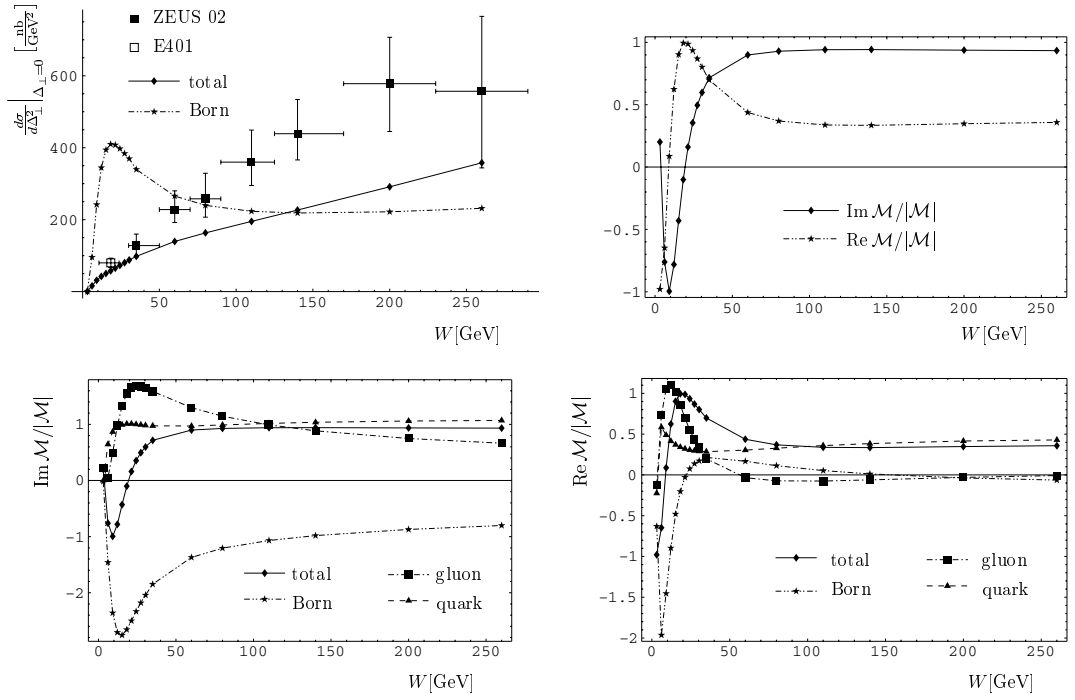

Fig. 17. The differential cross section for J/ψ photoproduction, NLO predictions for $\mu_F = \mu_R = 1.52\,\mathrm{GeV}$, and the data from E401 [1] and ZEUS [7]. The labeling of the curves is the same as in Fig. 15

Note that all steps of the dispersion method developed in this paper can be applied directly to NLO electroproduction, the process of a heavy vector meson being produced by a virtual photon. In this case the calculations may be much more involved due to the presence of an additional parameter, namely m/Q. However, for electroproduction the photon virtuality shifts the hard scale to the higher values in comparison to photoproduction. This gives hope that the factorization approach may be reliable for electroproduction of J/Ψ starting from some, not too high, values of Q.

We show, see (3.74) and (3.75), that convolution of the NLO hard-scattering amplitudes with GPDs produces contributions which are parameterically enhanced at high energies, $\sim \alpha_S^2 \ln(1/\xi)$. These contributions originate from the diagrams of partonic subprocess with gluon exchange in the t-channel and are related to the s-channel radiation of an intermediate parton in the wide interval of rapidity, away from the photon fragmentation region. In higher orders such radiation generates contributions $\sim \alpha_S(\alpha_S \ln(1/\xi))^n$. The $k_\perp$ factorization approach allows us to sum this class of logarithmic corrections to all orders in α_S, consistently with the fixed-order factorization of the collinear singularities [50]. It would be very interesting to perform such studies for heavy vector meson production. We believe that a resummation of these contributions will lead to much more stable theoretical predictions at high energies.

Acknowledgements. We are grateful to A. Freund for providing us with the code for the generalized parton distributions. Work of D.I. is supported in part by Alexander von Humboldt Foundation, by BMBF and by DFG 436 grant and by RFBR 02-02-17884. L.Sz. is partially supported by the French-Polish scientific agreement Polonium.

References

1. M. Binkley et al., Phys. Rev. Lett. **48**, 73 (1982)
2. B.H. Denby et al., Phys. Rev. Lett. **52**, 795 (1984)
3. S. Aid et al. [H1 Collaboration], Nucl. Phys. B **472**, 3 (1996) [hep-ex/9603005]
4. J. Breitweg et al. [ZEUS Collaboration], Z. Phys. C **75**, 215 (1997) [hep-ex/9704013]
5. J. Breitweg et al. [ZEUS Collaboration], Phys. Lett. B **437**, 432 (1998) [hep-ex/9807020]
6. C. Adloff et al. [H1 Collaboration], Phys. Lett. B **483**, 23 (2000) [hep-ex/0003020]
7. S. Chekanov et al. [ZEUS Collaboration], Eur. Phys. J. C **24**, 345 (2002) [hep-ex/0201043]
8. S. Aid et al. [H1 Collaboration], Nucl. Phys. B **468**, 3 (1996) [hep-ex/9602007]
9. J. Breitweg et al. [ZEUS Collaboration], Eur. Phys. J. C **6**, 603 (1999) [hep-ex/9808020]
10. M.G. Ryskin, Z. Phys. C **57**, 89 (1993)
11. S.J. Brodsky, L. Frankfurt, J.F. Gunion, A.H. Mueller, M. Strikman, Phys. Rev. D **50**, 3134 (1994) [hep-ph/9402283]
12. A.V. Radyushkin, Phys. Lett. B **385**, 333 (1996) [hep-ph/9605431]
13. X.D. Ji, Phys. Rev. Lett. **78**, 610 (1997) [hep-ph/9603249]
14. X.D. Ji, Phys. Rev. D **55**, 7114 (1997) [hep-ph/9609381]
15. A.V. Radyushkin, Phys. Lett. B **380**, 417 (1996) [hep-ph/9604317]
16. J.C. Collins, L. Frankfurt, M. Strikman, Phys. Rev. D **56**, 2982 (1997) [hep-ph/9611433]

17. M. Burkhardt, Phys. Rev. D **62**, 071503 (2000), Erratum D **66**, 119903 (2002) [hep-ph/0005108]
18. M. Diehl, Eur. Phys. J. C **25**, 223 (2002) Erratum C **31**, 277 (2003) [hep-ph/0205208]
19. A.V. Belitsky, Xiang-dong Ji, Feng Yuan, hep-ph/0307383
20. K. Goeke, V. Polyakov, M. Vanderhaeghen, Prog. Part. Nucl. Phys. **47**, 401 (2001) [hep-ph/0106012]
21. M. Diehl, Phys. Rept. **388**, 41 (2003) [hep-ph/0307382]
22. S. Catani, M. Ciafaloni, F. Hautmann, Nucl. Phys. B **366**, 135 (1991)
23. J.C. Collins, R.K. Ellis, Nucl. Phys. B **360**, 3 (1991)
24. E.A. Kuraev, L.N. Lipatov, V.S. Fadin, Sov. Phys. JETP **45**, 199 (1977) [Zh. Eksp. Teor. Fiz. **72**, 377 (1977)]
25. I.I. Balitsky, L.N. Lipatov, Sov. J. Nucl. Phys. **28**, 822 (1978) [Yad. Fiz. **28**, 1597 (1978)]
26. N.N. Nikolaev, B.G. Zakharov, Z. Phys. C **49**, 607 (1991)
27. A.H. Mueller, Nucl. Phys. B **415**, 373 (1994)
28. V.S. Fadin, L.N. Lipatov, Phys. Lett. B **429**, 127 (1998) [hep-ph/9802290]
29. B. Andersson et al. [Small x Collaboration], Eur. Phys. J. C **25**, 77 (2002) [hep-ph/0204115]
30. J. Nemchik, N.N. Nikolaev, B.G. Zakharov, Phys. Lett. B **341**, 228 (1994) [hep-ph/9405355]
31. M.G. Ryskin, R.G. Roberts, A.D. Martin, E.M. Levin, Z. Phys. C **76**, 231 (1997) [hep-ph/9511228]
32. L. Frankfurt, W. Koepf, M. Strikman, Phys. Rev. D **57**, 512 (1998) [hep-ph/9702216]
33. A.D. Martin, M.G. Ryskin, T. Teubner, Phys. Lett. B **454**, 339 (1999) [hep-ph/9901420]
34. L.L. Frankfurt, M.F. McDermott, M. Strikman, JHEP **9902**, 002 (1999) [hep-ph/9812316]
35. J. Hüfner, Y.P. Ivanov, B.Z. Kopeliovich, A.V. Tarasov, Phys. Rev. D **62**, 094022 (2000) [hep-ph/0007111]
36. A.C. Caldwell, M.S. Soares, Nucl. Phys. A **696**, 125 (2001) [hep-ph/0101085]
37. E. Gotsman, E. Ferreira, E. Levin, U. Maor, E. Naftali, Phys. Lett. B **503**, 277 (2001) [hep-ph/0101142]
38. J.P. Ma, J.S. Xu, Nucl. Phys. B **640**, 283 (2002) [hep-ph/0111391]
39. G.T. Bodwin, E. Braaten, G.P. Lepage, Phys. Rev. D **51**, 1125 (1995) Erratum D **55**, 5853 (1997) [hep-ph/9407339]
40. R. Barbieri, R. Gatto, R. Kogerler, Z. Kunszt, Phys. Lett. B **57**, 455 (1975)
41. P. Hoodbhoy, Phys. Rev. D **56**, 388 (1997) [hep-ph/9611207]
42. M. Vanttinen, L. Mankiewicz, Phys. Lett. B **434**, 141 (1998) [hep-ph/9805338]
43. D.Yu. Ivanov, L. Szymanowski, hep-ph/0312082
44. F.E. Low, Phys. Rev. **110**, 974 (1958)
45. E. Braaten, J. Lee, Phys. Rev. D **67**, 054007 (2003) [hep-ph/0211085]
46. V.M. Braun, D.Yu. Ivanov, A. Schäfer, L. Szymanowski, Nucl. Phys. B **638**, 111 (2002) hep-ph/0204191
47. D.J. Broadhurst, N. Gray, K. Schilcher, Z. Phys. C **52**, 111 (1991)
48. A. Freund, M. McDermott, M. Strikman, Phys. Rev. D **67**, 036001 (2003) [hep-ph/0208160]
49. J. Pumplin, D.R. Stump, J. Huston, H.L. Lai, P. Nadolsky, W.K. Tung, JHEP **0207**, 012 (2002) [hep-ph/0201195]
50. S. Catani, F. Hautmann, Nucl. Phys. B **427**, 475 (1994) [hep-ph/9405388]